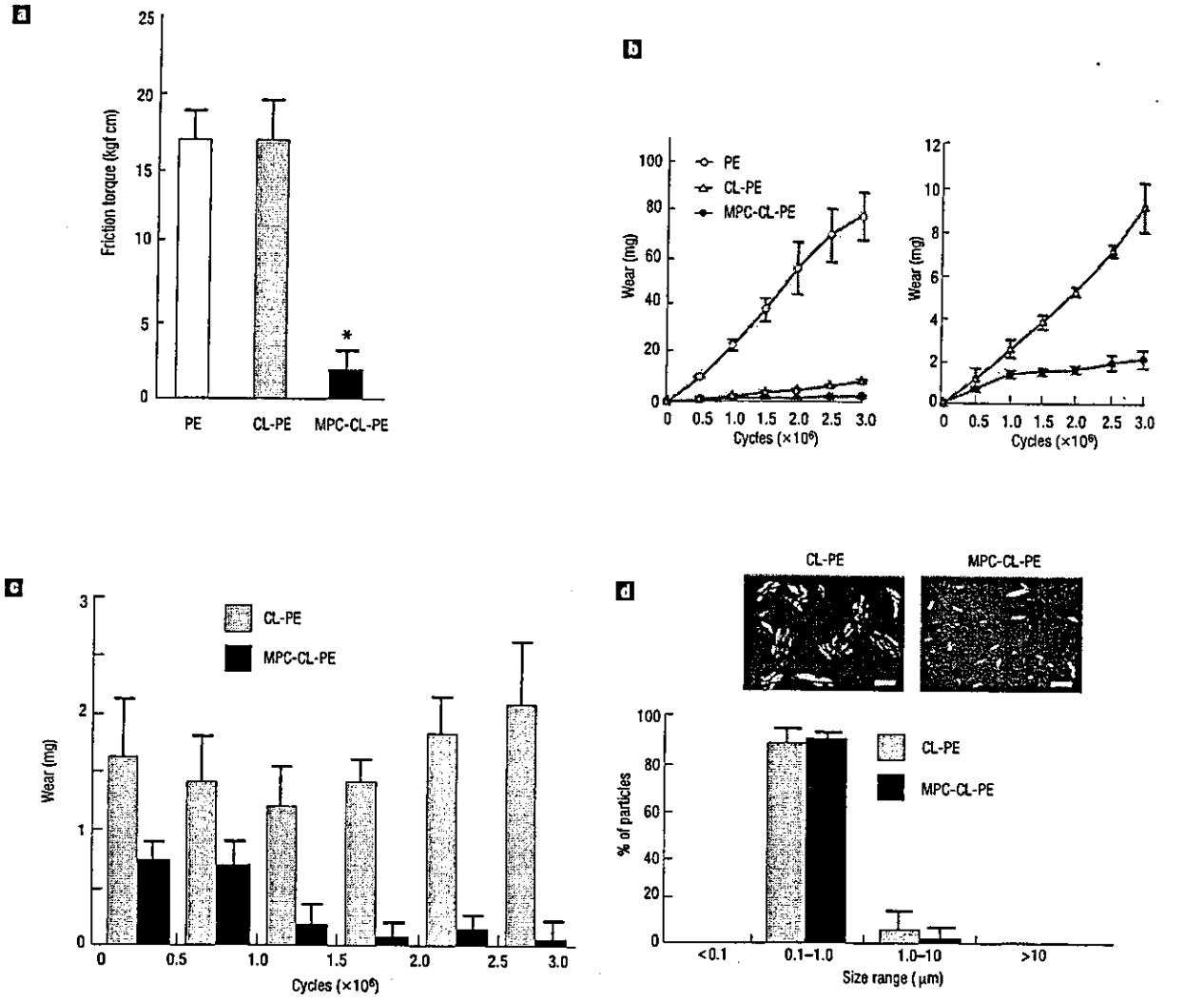

Figure 2 The friction torque and the wear amount in the hip-joint simulator with three kinds of PE liners. **a**, Friction torque of the three liners against the femoral heads measured before the loading test. **b**, Time course of the wear amount produced from the three liners during 3×10^6 cycles of loading. The CL-PE and MPC-CL-PE data are shown in an expanded scale on the right. **c**, The wear amount from the CL-PE and MPC-CL-PE liners for every 5×10^5 cycle intervals. **d**, Representative SEM images of the wear particles isolated from lubricants of the simulators with CL-PE and MPC-CL-PE liners. The graph below shows the distribution of particles in each size range. Data are expressed as means (symbols and bars) ± s.e.m. (error bars) for 10 liners per group. * significant difference from PE; $P<0.01$.

bond and the ester bond, respectively, and those in the nitrogen atom at 403 eV (N_{1s}) and phosphorus atom at 133 eV (P_{2p}) were specific to the phosphorylcholine group in the MPC unit.

To assess the lubricity and hydrophilicity, the MPC was grafted onto the PE plate (MPC-PE plate). The friction coefficient measured using a tensile test device and the contact angle of a water drop measured using the sessile drop method with a goniometer on the MPC-PE plate were about 1/7 and 1/5, respectively, of those on the non-grafted PE plate (Fig. 1c,d). These results indicate that the MPC grafting on PE greatly increases both lubricity and hydrophilicity.

Mechanical effects of the MPC grafting on the hip prosthesis were examined using a hip-joint wear simulator[16] under the conditions recommended by the International Organization for Standardization (ISO). We prepared crosslinked acetabular PE liners with photoinduced grafting of MPC onto their surface (MPC-CL-PE liner), and compared them with crosslinked PE liners without the MPC grafting (CL-PE liner) and non-crosslinked PE liners without the MPC grafting (PE liner). The friction torques of the three liners against the femoral head were compared before the loading test. There was no difference between PE and CL-PE liners; however, the MPC-CL-PE liner showed 80–90% lower torque than these two (Fig. 2a). Throughout the 3×10^6 cycles of gravimetric loading by the hip-joint simulator, the wear amount of the MPC-CL-PE liner was about 4 and 40 times less than those of the CL-PE and the PE liners, respectively (Fig. 2b). Clinically, the wear rate at the initial stage after a total hip replacement is thought to be well correlated with the incidence of periprosthetic osteolysis, because the wear particles may gain access to the articulation and accelerate the additional wear by a three-body mechanism[17]. In fact, the time-course analysis of the wear amount for every 5×10^5 cycle intervals

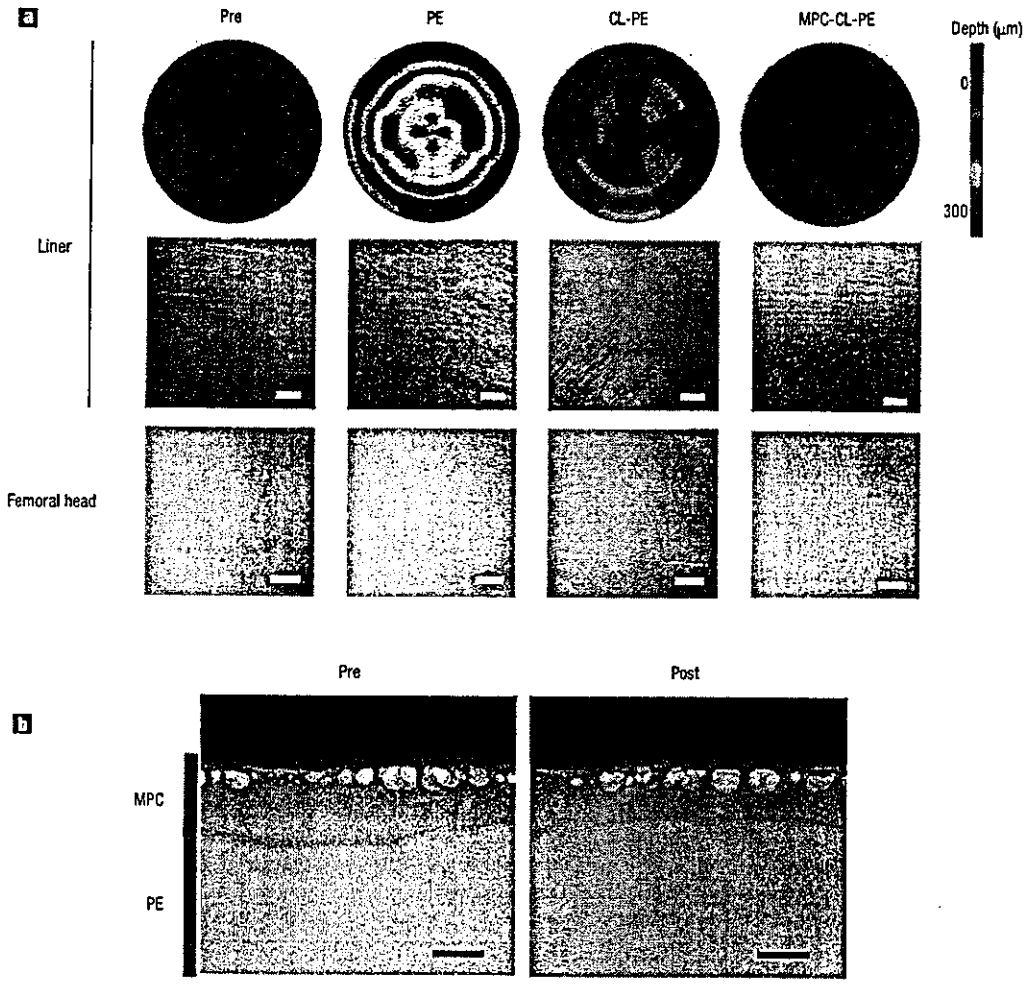

Figure 3 Optical findings of the surfaces of liners and corresponding femoral heads. a, Three-dimensional morphometric and SEM analyses of the liner surfaces (top and middle, respectively) and SEM analyses of the femoral head surfaces (bottom) before (Pre) and after 3×10^6 cycles of loading. Scale bars, 500 μm and 20 μm in middle and bottom, respectively. **b**, FE-TEM images of the thickness of MPC layer before (Pre) and after (Post) the loading. The bubbles on the surface were produced in the process of preparing the specimen. Scale bars, 100 nm.

revealed that the amount from the CL-PE liner was about twice as large as that from the MPC-CL-PE in the initial cycles, and somewhat increased in the later cycles (Fig. 2c). Contrarily, about 70% of the total wear amount was produced from the MPC-CL-PE liner in the initial 1×10^6 cycles, and decreased thereafter. In the last 5×10^5 cycles, the wear amount of MPC-CL-PE was less than 1/20 that of CL-PE. Although the present 3×10^6 cycles of 280 kgf (kilogram force) load is assumed equivalent to 3–10 years of physical walking, this result suggests that the mechanical effect of the MPC grafting will be maintained or somewhat more pronounced even after loading beyond 3×10^6 cycles. In fact, our preliminary simulator experiment with 1×10^7 cycles of loading revealed much stronger wear resistance by this grafting (data not shown). Scanning electron microscopy (SEM; JSM-5800LV, JEOL, Tokyo, Japan) analysis of the wear particles isolated from the lubricants revealed no significant difference of the particle size distribution between CL-PE and MPC-CL-PE liners, the great majority of which was 0.1–1.0 μm (Fig. 2d).

Optical examination of the liner surface using a three-dimensional morphometric analysis after 3×10^6 cycles of loading revealed that there was little or no wear in the MPC-CL-PE liner, whereas substantial wear was detected in the PE and CL-PE liners (Fig. 3a, top). The SEM analysis of the liner surface revealed that the original machine marks by the manufacturer's processing still remained on the MPC-CL-PE liner surface, which were completely obliterated in the two control liners (Fig. 3a, middle). Furthermore, the field emission transmission electron microscopy (FE-TEM) analysis showed that most of the liner surface was covered by the MPC polymer layer even after 3×10^6 cycles of loading (Fig. 3b). The XPS analysis also confirmed the remainder of the specific spectra of C_{1s}, P_{2p} and N_{1s} on the MPC-PE liner surface just as in Fig. 1b after the loading (data not shown). Contrarily, the SEM analysis of the femoral head showed no difference among the three groups (Fig. 3a, bottom). The femoral heads were free of visible scratches and the surface roughness expressed by the R_a values was not different before or after the loading in all groups (R_a = 0.05–0.06 μm), suggesting there was no abrasive contamination with metal particles from the heads in the hip-joint simulator.

With respect to the reduction of wear by the MPC grafting, we should consider the lubrication mechanism between the liners and

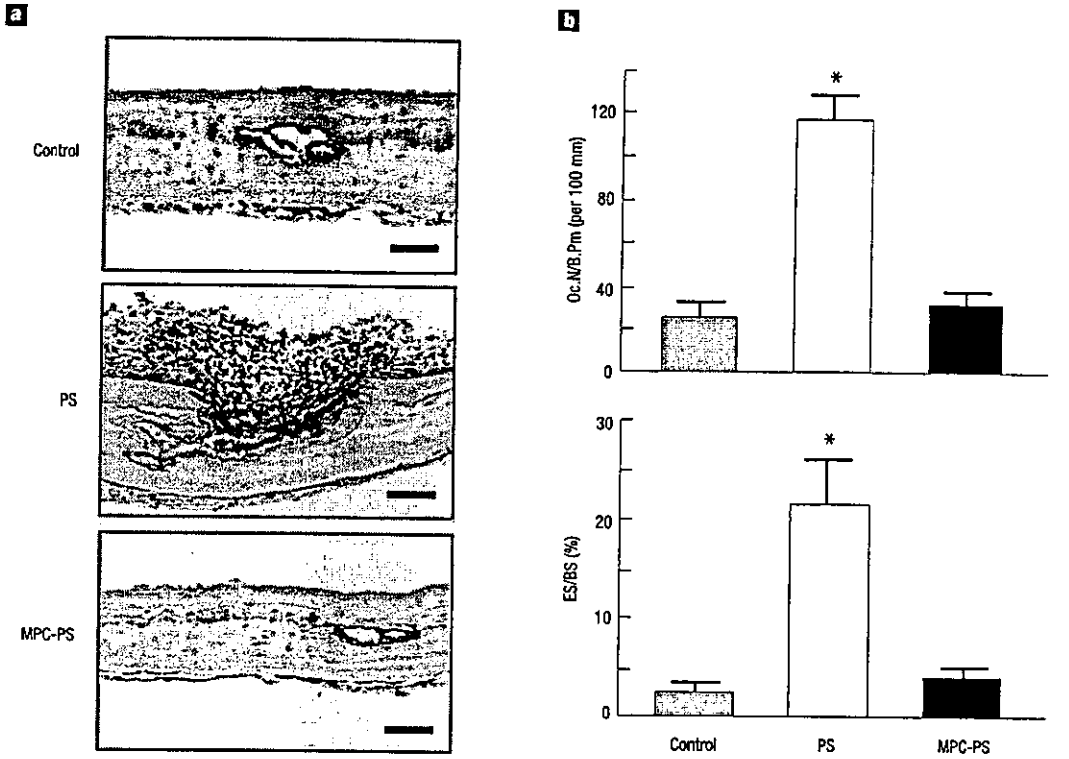

Figure 4 ***In vivo*** **bone resorption in mouse calvariae.** Resorption induced by a subperiosteal injection of an aliquot of PS particles with and without the MPC grafting (MPC-PS and PS, respectively) or an equal volume of solvent alone (control). a, Representative histological findings of the injected sites where osteoclasts were stained red with TRAP. Scale bars, 100 μm. b, Histomorphometric analyses of the injected sites: number of mature osteoclasts in 100 mm of bone perimeter (Oc.N/B.Pm; top) and percentage of eroded surfaces (ES) / bone surfaces (BS) (bottom). Data are expressed as means (bars) ± s.e.m. (error bars) for 8 calvariae per group. * significant difference from control; $P<0.01$.

metal heads of the hip-joint simulator. Although phospholipids themselves are known to work as effective boundary lubricants[18,19], recent studies of natural synovial joints have shown that fluid film lubrication by the intermediate hydrated layer is the predominant mechanism under physiological walking conditions[20]. Because the present study revealed that the MPC grafting onto the PE plate increased the hydrophilicity (Fig. 1d) and our previous study showed that the free-water fraction on the MPC polymer surface is kept at a higher level[21], the reduction of wear is likely to arise from the hydrated lubricating layer that is formed by the MPC grafting.

As PE particles are known to be most abundant and catabolic among wear particles in the periprosthetic tissues[3–5], alternative bearing surfaces have been proposed such as ceramic-on-ceramic and metal-on-metal articulations; however, these have their own potential disadvantages[22,23]. The long history and popularity of PE as a bearing surface has led to research in the development of tougher and more wear-resistant PE materials: the incorporation of short chopped carbon fibres in PE matrix (Poly II)[3,24], the extension of chain crystallite morphology with thicker lamellae and higher crystallinity (Hylamer)[25], and the creation of a three-dimensional molecular network by the crosslinking. Among them, only the crosslinking successfully improved the wear resistance and suppressed the periprosthetic osteolysis in the clinical setting[26,27]. It is therefore noteworthy that the MPC grafting onto the crosslinked PE surface further increased the wear resistance over the conventional crosslinked PE.

Considering that MPC is a biocompatible polymer, we next examined biological responses to particles using *in vivo* and *in vitro* models. The MPC polymer was grafted using a solvent-evaporation technique onto the surface of polystyrene (PS) particles whose size was approximately 500 nm in diameter, based on the result above (Fig. 2d) and previous findings[5,28] that the mean particle size from clinically failed prostheses is around 500 nm with >90% of particles less than 1 μm. The XPS spectra of C_{1s}, P_{2p} and N_{1s} on the surface of the PS particles grafted with MPC were quite similar to that of the MPC-PE liner surface as shown in Fig. 1b (data not shown). Although the surface electrical potential (ζ-potential) of the surface of non-grafted PS particles determined using electrophoretic light scattering was around −66.0 mV, the MPC grafting neutralized the potential to −2.5 mV, as we reported previously[29]. These results indicate that the MPC polymer was stably immobilized on the surface of the particles.

We first compared the *in vivo* bone resorption induced by PS particles with and without the MPC grafting using an established *in vivo* murine calvarial model[7,30]. When non-treated PS particles were injected beneath the calvarial periosteum, notable stimulations of tartrate-resistant acid phosphatase (TRAP)-positive osteoclast formation and bone resorption with inflammatory reaction were observed (Fig. 4a). However, subperiosteal injection of the MPC-grafted particles did not induce bone resorption. This effect was confirmed by histomorphometric analysis: the osteoclast number and the eroded surface of the calvarial bone that were increased

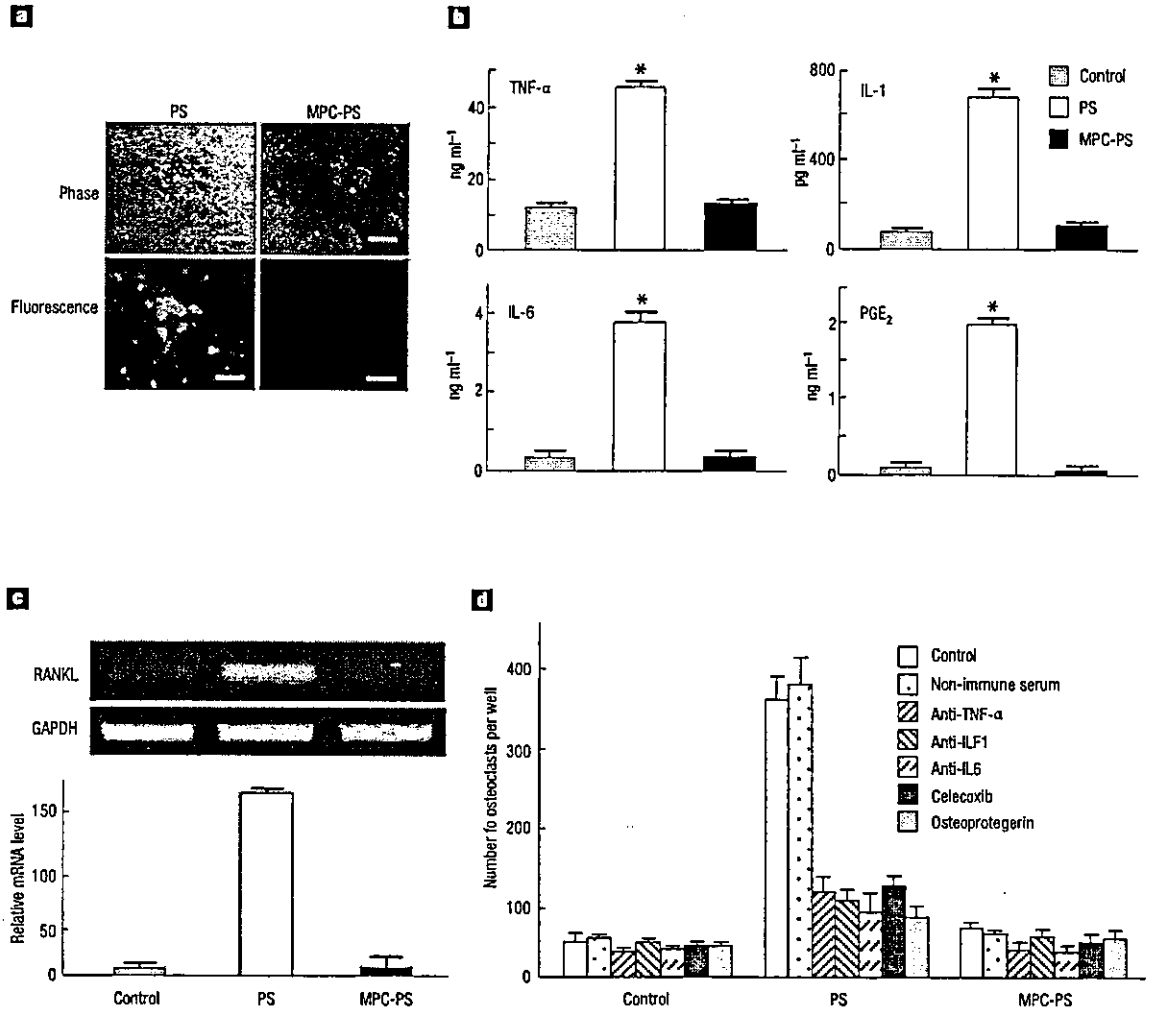

Figure 5 Bone-resorptive responses in cultures exposed to PS particles with and without the MPC grafting (MPC-PS and PS, respectively). a, Phagocytosis of fluorescence-labelled particles by cultured mouse intraperitoneal macrophages. Phase: phase contrast microscopic image. Fluorescence: fluorescence microscopic image. Scale bars, 100 μm. **b,** Concentrations of bone-resorptive factors TNF-α, IL-1, IL-6 and PGE_2 in the supernatants of the mouse macrophage-like cell line J774 culture with or without exposure to particles. **c,** RANKL expression by mouse primary osteoblasts isolated from neonatal mouse calvariae and cultured in the three kinds of conditioned media of the J774 cell cultures above. RANKL mRNA levels were determined by semiquantitative RT-PCR (top) and real-time RT-PCR (bottom). GAPDH is glyceraldehyde 3-phosphate dehydrogenase. **d,** Osteoclastogenesis in the coculture of mouse bone marrow cells and osteoblasts by the three kinds of conditioned media of J774 cells above, and inhibition by antagonists to cytokines, PGs and RANKL. Osteoclastogenesis was determined by the number of TRAP-positive multinucleated cells. Data are expressed as means (bars) ± s.e.m. (error bars) for 8–12 cultures per group. * significant difference from control; $P<0.01$.

four- to sixfold by the implantation of non-treated PS particles, as compared with those by the solvent alone, but were little affected by the MPC-grafted particles, indicating that MPC grafting is biologically inert (Fig. 4b).

To further investigate the cellular and molecular mechanisms underlying the prevention of osteoclastic bone resorption by the MPC grafting, we first compared the phagocytosis of fluorescence-labelled PS particles with and without the MPC grafting by cultured mouse intraperitoneal macrophages. Although large amounts of non-treated particles were phagocytosed by macrophages, the MPC-grafted particles were not taken into the cells, probably because biocompatible MPC polymer prevented macrophages from recognizing the particles as foreign bodies (Fig. 5a). We next examined the secretion of bone-resorptive factors by macrophages exposed to the particles. Concentrations of TNF-α, IL-1, IL-6 and PGE_2 in the culture medium of mouse macrophage-like cell line J774 cells were 4–20 times more stimulated by the exposure to non-treated PS particles than those without the exposure; however, the exposure to the MPC-grafted particles affected none of them (Fig. 5b). When the conditioned media of J774 cells were added to a mouse osteoblast culture, the receptor of NF-kB ligand (RANKL) was strongly expressed by the medium exposed to non-treated particles, but not by that exposed to the MPC-grafted particles (Fig. 5c). These results indicate that the MPC grafting prevented the secretion of resorptive factors by macrophages and the subsequent RANKL expression by osteoblasts. Finally, osteoclastogenesis in the coculture of mouse bone marrow cells and osteoblasts was increased about sevenfold by the conditioned medium of J774 cells exposed

to non-treated PS particles as compared with the control, and this stimulation was significantly inhibited by addition of anti-TNF-α, anti-IL-1 or anti-IL-6 antibody, a cyclooxygenase-2 (COX-2) inhibitor celecoxib, and a RANKL inhibitor osteoprotegerin; this confirmed the involvement of some network systems of these factors in the osteoclastogenesis by wear particles. Contrarily, the conditioned medium of J774 cells exposed to the MPC-grafted particles did not increase osteoclastogenesis (Fig. 5d). These biological findings indicate that the MPC grafting can successfully inhibit the bone-resorptive response to wear particles to levels similar to those of recently developed pharmacological therapies such as cytokine antagonists, COX-2 inhibitors and osteoprotegerin[7,8]. Because the lack of side effects of the MPC grafting has already been confirmed clinically by several medical devices[12–14], this surface grafting will surpass the pharmacologic therapies that possibly cause serious side effects during a long period of administration after surgery.

For these biological studies, we initially tried to use the PE wear particles isolated from the hip-simulator experiment above; however, it turned out to be impossible because the PE particles could not be isolated from the lubricants without damaging the MPC polymer layer. The lubricants after loading contain abundant and adhesive proteins that were degraded and precipitated by the heat generated by the head-liner friction. For the isolation of PE particles, it is essential to digest the proteins using strong hydroxide[28,31,32], which cannot avoid breaking the chemical structure such as the esteratic bond of the MPC unit. In fact, the XPS analysis of the surface of isolated particles revealed the lack of the MPC polymer layer. In addition, even if we could isolate the PE particles with MPC grafting properly, the amount from the MPC-CL-PE liner was too small to be used for the biological experiments. We therefore attempted to graft MPC onto the surface of new PE particles or the wear particles from the simulator experiment; however, the floating nature of PE on the liquid surface due to the low specific gravity made the photoinduced polymerization of MPC impossible, because the grafting procedure requires that the particles be agitated in the liquid[29]. Hence, for the biological experiments we used PS particles that have conventionally been used for the *in vivo* and *in vitro* analyses of particle-induced osteolysis as a substitute for PE[6,33,34]. PS is a hydrocarbon polymer just like PE, but has a higher specific gravity than PE. Because these two polymers share similar physical and chemical properties—electrically neutral and little chemical sensitivity—we believe that biological responses to these particles are also similar.

Taken together, the present results demonstrate that grafting MPC onto the PE liner surface of the hip prosthesis markedly decreased the friction and the production of wear particles. In addition, even if the particles were produced by friction, they were biologically inert with respect to phagocytosis by macrophages and subsequent bone-resorptive responses: secretion of cytokines and PGE_2, induction of RANKL, and osteoclastogenesis.

Although this study focused on the hip prosthesis, whose loosening is the most frequent and serious among total joint replacements of upper and lower extremities, the MPC grafting can be used for the prevention of periprosthetic osteolysis of other joints, in which PE particles from articular interfaces are also known to initiate the catabolic cascade[35,36]. From the mechanical and biological advantages shown in this study, we believe that the MPC grafting will make a significant improvement in total joint replacements by preventing periprosthetic osteolysis and aseptic loosening. The development of this technique would improve the quality of care of patients having total joint replacements and have a substantial public health impact. We are now designing a large-scale clinical trial.

METHODS

For mechanical analyses, a 12-station hip-joint wear simulator apparatus (MTS, MTS Systems, Minneapolis, Minnesota) with three kinds of PE liners in 42 mm acetabular cups: non-crosslinked PE liner (K-MAX, Japan Medical Materials, Osaka), crosslinked PE liner (K-MAX Excellink), and MPC-grafted K-MAX Excellink, coupled to 22 mm cobalt–chromium–molybdenum alloy heads (K-MAX HH-02, Excellink), was mounted on rotating blocks to produce biaxial or orbital motion[14]. The simulator experiment was performed according to the international standard of "implants for surgery – wear of total hip-joint prosthesis" established by ISO (#14242-1; 2002), which was proved to be closest to the physiological conditions. Briefly, a Paul-type loading profile, which is a physiological walking simulation with continuous cyclic motion and loading, was applied (maximum force = 280 kgf, frequency = 1 Hz)[37] in the lubricant of distilled water containing 25% bovine calf serum. Friction torque between the liner and the femoral head was measured using a torque measuring instrument. The simulator was run up to 3×10^6 cycles, and the change of lubricant and gravimetric measurement of the liners were performed every 5×10^5 cycles. For the isolation of wear particles, the lubricant after the loading was incubated with 5 N NaOH solution in order to digest adhesive proteins that were degraded and precipitated; the particles were then collected and underwent sequential filtrations, as reported previously[33]. The size of particles was defined as the maximum dimensions by SEM analysis.

For biological analyses, all animal experiments were performed according to the guidelines of the International Association for the Study of Pain[38], and were approved by the committee of Tokyo University charged with confirming ethics. The *in vivo* mouse calvaria experiment was performed as reported previously[7,28]. Briefly, after exposing the calvaria of mice, a subperiosteal injection of PS particles (average diameter = 468 nm; Polysciences, Warrington, Pennsylvania) with or without the MPC grafting, or an equal volume of solvent (deionized water) alone was performed.

Mice were sacrificed seven days after the surgery, and the calvaria was excised, fixed, and decalcified in EDTA. Osteoclastogenesis in the coronal histological sections was determined by TRAP staining. The sections were subjected to histomorphometric analyses under a light microscope with a micrometer, and parameters for bone resorption were measured as reported previously[39]. For the phagocytosis experiment, mouse intraperitoneal macrophages were isolated, exposed to fluorescence-labelled particles, cultured for 1 h, and observed with a fluorescence microscope. Mouse macrophage-like cell line J774 cells (Riken Cell Bank, Saitama, Japan) were exposed to particles and cultured for 24 h. The supernatants were subject to cytokine and PGE_2 measurements using the ELISA method, and were used as the conditioned media for the following assays. For the RANKL expression assay, mouse osteoblasts isolated from neonatal calvariae were cultured in the conditioned media for 24 h. RANKL expression in osteoblasts was measured using the semi-quantitative and real-time reverse transcription polymerase chain reaction (RT-PCR) analyses. The information on the primers is available upon request. For osteoclast formation assay, mouse primary osteoblasts above and bone marrow cells isolated from adult mouse long bones were cocultured in the conditioned media in the presence or absence of anti-TNF-α, anti-IL1, anti-IL-6 antibody, control non-immune serum, celecoxib or osteoprotegerin. Cells were stained with TRAP, and those positively stained and containing more than three nuclei were counted as osteoclasts. For the statistical analysis, means of groups were compared by ANOVA and the significance of differences was determined by post-hoc testing using Bonferroni's method.

Received 13 April 2004; accepted 9 Augsut 2004; published 24 October 2004.

References

1. Harris, W. H. Wear and periprosthetic osteolysis: the problem. *Clin. Orthop.* 393, 66–70 (2001).
2. Jacobs, J. J., Roebuck, K. A., Archibeck, M., Hallab, N. J. & Glant, T. T. Osteolysis: basic science. *Clin. Orthop.* 393, 71–77 (2001).
3. Connelly, G. M., Rimnac, C. M., Wright, T. M., Hertzberg, R. W. & Manson, J. A. Fatigue crack propagation behavior of ultrahigh molecular weight polyethylene. *J. Orthop. Res.* 2, 119–125 (1984).
4. von Knoch, M. *et al.* The effectiveness of polyethylene versus titanium particles in inducing osteolysis in vivo. *J. Orthop. Res.* 22, 237–243 (2004).
5. Maloney, W. J. *et al.* Isolation and characterization of wear particles generated in patients who have had failure of a hip arthroplasty without cement. *J. Bone Joint Surg. Am.* 77, 1301–1310 (1995).
6. Glant, T. T. *et al.* Bone resorption activity of particulate-stimulated macrophages. *J. Bone Miner. Res.* 8, 1071–1079 (1993).
7. Childs, L. M. *et al.* In vivo RANK signaling blockade using the receptor activator of NF-κB:Fc effectively prevents and ameliorates wear debris-induced osteolysis via osteoclast depletion without inhibiting osteogenesis. *J. Bone Miner. Res.* 17, 192–199 (2002).
8. Goater, J. J., O'Keefe, R. J., Rosier, R. N., Puzas, J. E. & Schwarz, E. M. Efficacy of ex vivo OPG gene therapy in preventing wear debris induced osteolysis. *J. Orthop. Res.* 20, 169–173 (2002).
9. Ishihara, K., Ueda, T. & Nakabayashi, N. Preparation of phospholipid polymers and their properties as polymer hydrogel membrane. *Polym. J.* 22, 355–360 (1990).
10. Ishihara, K., Shinozuka, T., Hanazaki, Y., Iwasaki, Y. & Nakabayashi, N. Improvement of blood compatibility on cellulose hemodialysis membrane: IV. Phospholipid polymer bonded to the membrane surface. *J. Biomater. Sci. Polym. Edn* 10, 271–282 (1999).
11. Yoneyama, T., Sugihara, K., Ishihara, K., Iwasaki, Y. & Nakabayashi, N. The vascular prosthesis without pseudointima prepared by antithrombogenic phospholipid polymer. *Biomaterials* 23, 1455–1459 (2002).
12. Kihara, S. *et al.* In vivo evaluation of a MPC polymer coated continuous flow left ventricular assist system. *Artif. Organs* 27, 188–192 (2003).
13. Lewis, A. L. Phosphorylcholine-based polymers and their use in the prevention of biofouling. *Colloids Surf. B* 18, 261–275 (2000).
14. Lewis, A. L., Tolhurst, L. A. & Stratford, P. W. Analysis of a phosphorylcholine-based polymer coating on a coronary stent pre- and post-implantation. *Biomaterials* 23, 1697–1706 (2002).
15. Ishihara, K., Iwasaki, Y., Ebihara, S., Shindo, Y. & Nakabayashi, N. Photoinduced graft polymerization of 2-methacryloyloxyethyl phosphorylcholine on polyethylene membrane surface for obtaining blood cell adhesion resistance. *Colloids Surf. B* 18, 325–335 (2000).
16. Nakamura, T. *et al.* Clinical and laboratory wear studies of zirconia-on-UHMWPE combination in cementless THA. *Key Eng. Mater.* 240–242, 823–826 (2003).
17. Sochart, D. H. Relationship of acetabular wear to osteolysis and loosening in total hip arthroplasty. *Clin. Orthop.* 363, 135–150 (1999).
18. Williams, P. F. 3rd, Powell, G. L. & LaBerge, M. Sliding friction analysis of phosphatidylcholine as a boundary lubricant for articular cartilage. *Proc. Inst. Mech. Eng. H* 207, 59–66 (1993).

19. Hills, B. A. Boundary lubrication in vivo. *Proc. Inst. Mech. Eng. H* 214, 83–94 (2000).
20. Dowson, D. & Jin, Z. M. Micro-elastohydrodynamic lubrication of synovial joints. *Eng. Med.* 15, 63–65 (1986).
21. Ishihara, K. *et al.* Why do phospholipid polymers reduce protein adsorption? *J. Biomed. Mater. Res.* 39, 323–330 (1998).
22. Black, J. Metal on metal bearings. A practical alternative to metal on polyethylene total joints? *Clin. Orthop.* 329, S244–S255 (1996).
23. Callaway, G. H., Flynn, W., Ranawat, C. S. & Sculco, T. P. Fracture of the femoral head after ceramic-on-polyethylene total hip arthroplasty. *J. Arthroplasty* 10, 855–859 (1995).
24. Wright, T. M., Rimnac, C. M., Faris, P. M. & Bansal, M. Analysis of surface damage in retrieved carbon fiber-reinforced and plain polyethylene tibial components from posterior stabilized total knee replacements. *J. Bone Joint Surg. Am.* 70, 1312–1319 (1988).
25. Livingston, B. J., Chmell, M. J., Spector, M. & Poss, R. Complications of total hip arthroplasty associated with the use of an acetabular component with a Hylamer liner. *J. Bone Joint Surg. Am.* 79, 1529–1538 (1997).
26. Kurtz, S. M., Muratoglu, O. K., Evans, M. & Edidin, A. A. Advances in the processing, sterilization, and crosslinking of ultra-high molecular weight polyethylene for total joint arthroplasty. *Biomaterials* 20, 1659–1688 (1999).
27. McKellop, H., Shen, F. W., DiMaio, W. & Lancaster, J. G. Wear of gamma-crosslinked polyethylene acetabular cups against roughened femoral balls. *Clin. Orthop.* 369, 73–82 (1999).
28. Ingram, J. H., Stone, M., Fisher, J. & Ingham, E. The influence of molecular weight, crosslinking and counterface roughness on TNF-alpha production by macrophages in response to ultra high molecular weight polyethylene particles. *Biomaterials* 25, 3511–3522 (2004).
29. Konno, T., Kurita, K., Iwasaki, Y., Nakabayashi, N. & Ishihara, K. Preparation of nanoparticles composed with bioinspired 2-methacryloyloxyethyl phosphorylcholine polymer. *Biomaterials* 22, 1883–1889 (2001).
30. Boyce, B. F., Aufdemorte, T. B., Garrett, I. R., Yates, A. J. & Mundy, G. R. Effects of interleukin-1 on bone turnover in normal mice. *Endocrinology* 125, 1142–1150 (1989).
31. Campbell, P. *et al.* Isolation of predominantly submicron-sized UHMWPE wear particles from periprosthetic tissues. *J. Biomed. Mater. Res.* 29, 127–131 (1995).
32. Jono, K., Takigawa, Y., Takadama, H., Mizuno, M. & Nakamura, T. A multi-station hip joint simulator study and wear characterization of commercial hip endoprostheses. *Ceram. Eng. Sci. Proc.* 24, 255–260 (2003).
33. Vermes, C. *et al.* The effects of particulate wear debris, cytokines, and growth factors on the functions of MG-63 osteoblasts. *J. Bone Joint Surg. Am. A* 83, 201–211 (2001).
34. Yao, J., Cs-Szabo, G., Jacobs, J. J., Kuettner, K. E. & Glant, T. T. Suppression of osteoblast function by titanium particles. *J. Bone Joint Surg. Am.* 79, 107–112 (1997).
35. Inagaki, K. *et al.* Importance of a radial head component in Sorbie unlinked total elbow arthroplasty. *Clin. Orthop.* 400, 123–131 (2002).
36. Shanbhag, A. S. *et al.* Quantitative analysis of ultrahigh molecular weight polyethylene (UHMWPE) wear debris associated with total knee replacements. *J. Biomed. Mater. Res.* 53, 100–110 (2000).
37. Paul, J. P. Forces transmitted by joints in the human body. *Proc. Inst. Mech. Eng.* 181, 8–15 (1967).
38. Zimmermann, M. Ethical guidelines for investigations of experimental pain in conscious animals. *Pain* 16, 109–110 (1983).
39. Ogata, N. *et al.* Insulin receptor substrate-1 in osteoblast is indispensable for maintaining bone turnover. *J. Clin. Invest.* 105, 935–943 (2000).

Acknowledgements

We thank Noboru Yamawaki, Takatoshi Miyashita, Hiroaki Takadama, Kaori Jono, Reiko Yamaguchi, and Mizue Ikeuchi for their excellent technical help. This work was supported by Grants-in-Aid for Scientific Research from the Japanese Ministry of Education, Culture, Sports, Science and Technology (#15390449), and Health and Welfare Research Grant for Comprehensive Research on Aging and Health from the Japanese Ministry of Health, Labour and Welfare.

Correspondence and requests for materials should be addressed to H.K.

Supplementary Information accompanies the paper on www.nature.com/naturematerials

Competing financial interests

The authors declare that they have no competing financial interests.

ARTHRITIS & RHEUMATISM
Vol. 50, No. 11, November 2004, pp 3561–3573
DOI 10.1002/art.20611

The Combination of SOX5, SOX6, and SOX9 (the SOX Trio) Provides Signals Sufficient for Induction of Permanent Cartilage

Toshiyuki Ikeda,[1] Satoru Kamekura,[2] Akihiko Mabuchi,[1] Ikuyo Kou,[1] Shoji Seki,[1] Tsuyoshi Takato,[3] Kozo Nakamura,[2] Hiroshi Kawaguchi,[2] Shiro Ikegawa,[1] and Ung-il Chung[3]

Objective. **To regenerate permanent cartilage, it is crucial to know not only the necessary conditions for chondrogenesis, but also the sufficient conditions. The objective of this study was to determine the signal sufficient for chondrogenesis.**

Methods. **Embryonic stem cells that had been engineered to fluoresce upon chondrocyte differentiation were treated with combinations of factors necessary for chondrogenesis, and chondrocyte differentiation was detected as fluorescence. We screened for the combination that could induce fluorescence within 3 days. Then, primary mesenchymal stem cells, nonchondrogenic immortalized cell lines, and primary dermal fibroblasts were treated with the combination, and the induction of chondrocyte differentiation was assessed by detecting the expression of the cartilage marker genes and the accumulation of proteoglycan-rich matrix. The effects of monolayer, spheroid, and 3-dimensional culture systems on induction by combinations of transcription factors were compared. The effects of the combination on hypertrophic and osteoblastic differentiation were evaluated by detecting the expression of the characteristic marker genes.**

Results. **No single factor induced fluorescence. Among various combinations examined, only the SOX5, SOX6, and SOX9 combination (the SOX trio) induced fluorescence within 3 days. The SOX trio successfully induced chondrocyte differentiation in all cell types tested, including nonchondrogenic types, and the induction occurred regardless of the culture system used. Contrary to the conventional chondrogenic techniques, the SOX trio suppressed hypertrophic and osteogenic differentiation at the same time.**

Conclusion. **These data strongly suggest that the SOX trio provides signals sufficient for the induction of permanent cartilage.**

Utilizing the differentiation and proliferation capabilities of stem cells, regenerative medicine attempts to treat irreversible organ failures that cannot be dealt with by conventional medical treatment. In the skeletal area, cartilage has a relatively poor regenerative capacity and, thus, may benefit most from regenerative medicine. Conditions such as osteoarthritis and congenital skeletal defects are apparent targets that have great medical and socioeconomic impact. To make cartilage regenerative medicine a reality, it is essential to know the conditions that are both necessary and sufficient for chondrogenesis.

A number of factors have been shown to be vital for chondrogenesis. These factors include the sex-determining region Y–type high mobility group box (SOX) family of transcription factors (1), insulin-like growth factor 1 (IGF-1) (2), fibroblast growth factor 2 (FGF-2) (3), Indian hedgehog (IHH) (4), bone morpho-

Dr. Ikegawa's work was supported by a grant from the Japanese Millennium Project and a Grant-in-Aid for Scientific Research from the Japanese Ministry of Education, Culture, Sports, Science, and Technology (14207055). Dr. Chung's work was supported by a Grant-in-Aid for Scientific Research from the Japanese Ministry of Education, Culture, Sports, Science, and Technology (15390452) and by a generous endowment from Takeda Chemical Industries, Osaka, Japan.

[1]Toshiyuki Ikeda, MD, Akihiko Mabuchi, MD, Ikuyo Kou, MEng, Shoji Seki, MD, Shiro Ikegawa, MD, PhD: SNP Research Center, RIKEN (The Institute of Physical and Chemical Research), Tokyo, Japan; [2]Satoru Kamekura, MD, Kozo Nakamura, MD, PhD, Hiroshi Kawaguchi, MD, PhD: University of Tokyo Graduate School of Medicine, Tokyo, Japan; [3]Tsuyoshi Takato, MD, PhD, Ung-il Chung, MD, PhD: University of Tokyo Hospital, Tokyo, Japan.

Address correspondence and reprint requests to Shiro Ikegawa, MD, PhD: Laboratory for Bone and Joint Diseases, SNP Research Center, RIKEN, c/o Institute of Medical Science, University of Tokyo, 4-6-1 Shirokanedai, Minato-ku, Tokyo 108-8639, Japan. E-mail: sikegawa@ims.u-tokyo.ac.jp.

Submitted for publication February 25, 2004; accepted in revised form August 2, 2004.

genetic protein 2 (BMP-2) (5), transforming growth factor β (TGFβ) (6), and Wnt proteins (4).

Many lines of evidence, both in vitro and in vivo, have shown that SOX proteins are necessary for chondrogenesis. SOX9 is expressed in all chondroprogenitors and chondrocytes except hypertrophic chondrocytes (7,8). Heterozygous mutations of *SOX9* cause a severe chondrodysplasia, known as campomelic dysplasia, in humans (9,10). Analysis of chimeric mice containing wild-type and *Sox9*-deficient cells showed that the mutant cells were excluded from chondrogenic mesenchymal condensation and failed to express chondrocyte-specific marker genes (11). SOX9 was shown to bind to and activate chondrocyte-specific enhancer elements in *Col2a1*, *Col9a1*, *Col11a2*, and *Aggrecan* in vitro (12–18). Conditional ablation of the *Sox9* gene in limb buds before mesenchymal condensation resulted in a complete absence of chondrocytes, whereas conditional ablation of *Sox9* after mesenchymal condensation resulted in a severe generalized chondrodysplasia (19). Two other members of the Sox family, Sox5 and Sox6, are also required for chondrogenesis. $Sox5^{-/-}$ and $Sox6^{-/-}$ mice show chondrodysplastic phenotypes and die at birth. $Sox5^{-/-}$ and $Sox6^{-/-}$ mice develop a severe, generalized chondrodysplasia characterized by a virtual absence of cartilage (20). In vitro studies have shown that Sox5 and Sox6 cooperate with Sox9 to activate the *Col2a1* enhancer in chondrogenic cells (21).

Although these lines of evidence demonstrate that these factors are necessary for chondrogenesis, no single factor has proved sufficient for the process. That is, we do not yet know what constitutes a sufficient signal for chondrogenesis. In the current study, we sought to determine the sufficient signal by screening various combinations of known factors that are necessary for chondrogenesis.

MATERIALS AND METHODS

Construction of plasmid vectors and adenoviruses. Combinations of known factors important for chondrogenesis were screened. These factors included SOX5, SOX6, SOX9, IGF-1, FGF-2, IHH, BMP-2, TGFβ, and Wnt proteins. For each signaling pathway, we constructed an adenovirus vector that stimulates the pathway (overexpression of the wild-type form or expression of the constitutively active form) as well as one that inhibits the pathway (expression of the dominant-negative form or RNA interference [RNAi] form).

We then stimulated the signaling and inhibition of each factor. SOX signaling was stimulated as described below. To stimulate SOX inhibition, we constructed adenoviruses expressing RNAi for SOX5, SOX6, and SOX9 (22). To stimulate IGF-1 signaling, we used an adenovirus expressing insulin receptor substrate 1 (IRS-1); to inhibit, we used one expressing a dominant-negative form of IRS-1 (23). To stimulate FGF signaling, we constructed an adenovirus expressing a constitutively active form of FGF receptor 3 (FGFR-3); to inhibit, we used one expressing RNAi for FGFR-3 (24). To stimulate IHH signaling, we constructed an adenovirus expressing constitutively active Smoothened (25); to inhibit, we used one expressing a repressor form of Gli-3 (26). To stimulate BMP signaling, we used an adenovirus expressing a constitutively active form of activin receptor–like kinase 6 (ALK-6); to inhibit, we used one expressing Smad6 (27). To stimulate TGFβ signaling, we used an adenovirus expressing a constitutively active form of ALK-5; to inhibit, we used one expressing Smad7 (27). To stimulate Wnt signaling, we constructed an adenovirus expressing a constitutively active form of T cell factor (TCF); to inhibit, we used one expressing a dominant-negative form of TCF (28).

As a control vector, we used the adenovirus expressing the β-galactosidase gene *lacZ*. Thus, for each signaling pathway, there were 3 adenoviruses (positive, negative, and neutral). To create combinations, one adenovirus from each signaling pathway was selected and mixed with another.

To create adenoviruses expressing SOX5, SOX6, and SOX9, full-length human *SOX5*, *SOX6*, and *SOX9* complementary DNA (cDNA) was amplified by polymerase chain reaction (PCR) and cloned into pEGFPC1 and pShuttle mammalian expression vectors (Clontech, Palo Alto, CA). We confirmed that the introduced green fluorescence protein (GFP) tags did not interfere with the activities of any SOX. PCR products were verified by DNA sequencing. Adenovirus vectors expressing SOX5, SOX6, and SOX9 were constructed with the AdenoX Expression system (Clontech), according to the manufacturer's instructions. Adenovirus vector expressing LacZ was provided by the manufacturer. Adenoviruses were packaged and amplified in HEK 293 cells and purified with an AdenoX virus purification kit (Clontech). The viral titers were estimated with an AdenoX rapid titer assay kit (Clontech).

Isolation and culture of cells. Mouse embryonic stem (ES) cells were isolated from blastocysts obtained from C57BL/6 mice expressing a GFP transgene engineered to be expressed specifically in chondrocytes (*Col2-GFP*), as previously described (29). *Col2-GFP* ES cells were cultured in high-glucose Dulbecco's modified Eagle's medium (DMEM; Sigma, St. Louis, MO) supplemented with β-mercaptoethanol (100 μM), leukemia inhibitory factor (1,000 units/ml), nonessential amino acids (1%), penicillin (50 units/ml), streptomycin (50 μg/ml), and fetal bovine serum (FBS; 15%) (JRH Biosciences, Lenexa, KS), as previously described (30). To generate *Col2-GFP* mice, the 6.3-kb *Col2a1* promoter region directing chondrocyte-specific expression was released from the plasmid p3000i3020Col2a1 (a generous gift from Dr. Benoit de Crombrugghe, M. D. Anderson Cancer Center, Houston, TX) and subcloned into the pEGFP-1 vector (Clontech). The *Col2-GFP* transgene was then excised and purified for microinjection. Pronuclear injection and subsequent selection of founders were performed as previously described (31).

Human mesenchymal stem cells (MSCs) and adult human dermal fibroblasts (DFs) were purchased from Cambrex (East Rutherford, NJ). Human MSCs were cultured in MSC growth medium at 37°C under 5% CO_2. Adult human DFs were cultured in high-glucose DMEM supplemented with

penicillin (50 units/ml), streptomycin (50 μg/ml), and FBS (10%).

HuH-7 cells (RCB1366) were obtained from the RIKEN Cell Bank (Tsukuba, Japan). HeLa cells (JCRB9004) were obtained from the JCRB Cell Bank (Osaka, Japan). HEK 293 cells were purchased from Clontech. All cell lines were cultured at 37°C under 5% CO_2 in high-glucose DMEM supplemented with penicillin (50 units/ml), streptomycin (50 μg/ml), and FBS (10%).

In vitro cartilage formation by *Sox* gene transfer. Embryoid bodies were formed by 3-dimensional (3-D) suspension culture for 5 days and subsequent 2-D adhesive culture on gelatin-coated plates for 3 days. Then, the embryoid bodies were transduced with adenoviruses expressing the various genes listed above, including the SOX trio at 100 multiplicities of infection (MOI). Chondrogenic differentiation was detected as fluorescence by confocal fluorescent microscopy.

For spheroid culture, human MSCs and adult human DFs were cultured in 100-mm dishes until confluency, and adenoviruses expressing the *SOX* genes were transduced at 50 MOI. Two days after transduction, cells were trypsinized and 500,000 cells per tube were gently centrifuged to form spheroids. Spheroids were cultured in serum-free high-glucose DMEM or in chondrogenic medium, which consisted of 300 ng/ml of BMP-2 (Yamanouchi, Tokyo, Japan) and 10 ng/ml of TGFβ3 (Techne, Princeton, NJ) in addition to high-glucose DMEM supplemented with $10^{-7}M$ dexamethasone, 50 μg/ml of ascorbate, 40 μg/ml of proline, 100 μg/ml of pyruvate, and 1× insulin–transferrin–selenium+1 (Sigma). Cells were collected at 3, 7, 14, and 21 days after spheroid formation for histochemical analyses and real-time PCR.

For analysis of monolayer-cultured human MSCs and adult human DFs, *SOX* genes were transduced at 50 MOI. Cells were collected at 5, 9, 16, and 23 days after transduction for real-time PCR. Three-dimensional culture on collagen gel was performed with 3-D Collagen Cell Culture system (Koken, Tokyo, Japan), according to the manufacturer's instructions. The transduced human MSCs and adult human DFs were trypsinized 2 days after transduction and seeded onto a DMEM-containing collagen gel at a density of 250,000 cells/cm^2 in 24-well plates and then cultured in serum-free DMEM. Cells were collected at 7, 14, and 21 days of 3-D culture. In each culture system, the medium was replaced every 3–4 days.

Transfections of HuH-7, HeLa, and HEK 293 cell lines with GFP-SOX expression vectors were performed with FuGENE 6 transfection reagent (Roche, Mannheim, Germany). In cotransfection, the same amount of total DNA was used, and all plasmids were added in an equal ratio.

Real-time PCR analysis. Total RNAs from cells were isolated with an RNeasy mini kit (Qiagen, Hilden, Germany), according to the manufacturer's instructions. All total RNA samples were treated with DNase I. Total RNAs (50 ng to 1 μg) were reverse-transcribed with MultiScribe reverse transcriptase (ABI, Foster City, CA) and random hexamers in a 50-μl reaction volume, according to the manufacturer's instructions, and 1 μl of each reverse transcriptase reaction was used as a template for the second-step SYBR Green real-time PCR. The full-length or partial-length cDNA of target genes, including PCR amplicon sequences, were amplified by PCR, cloned into pCR-TOPO Zero II or pCR-TOPO II vectors (Invitrogen, Carlsbad, CA), and used as standard templates after linearization. QuantiTect SYBR Green PCR Master Mix (Qiagen) was used for the second-step SYBR Green real-time PCR according to the manufacturer's instructions. SYBR Green PCR amplification and real-time fluorescence detection were performed with an ABI 7700 Sequence Detection system. All reactions were run in quadruplicate. Copy numbers of target gene messenger RNA (mRNA) in each total RNA were calculated by reference to standard curves and were adjusted to the human or mouse standard total RNA (ABI) with the human GAPDH or rodent Gapdh as an internal control.

Each primer position in the coding sequences of target genes is described below. SOX5 and SOX6 primer sets were designed on the N-terminal domain of their long isoforms. The human set was as follows: for aggrecan, 6497–6796; for chondromodulin 1, 175–431; for COL2A1, 3856–4123; for COL9A1, 338–635; for COL10A1, 1641–1843; for COL11A2, 2543–2836; for matrilin 3, 232–422; for SOX5, 354–854; for SOX6, 315–593; for SOX9, 651–762; for RUNX2, 1270–1447; for COL1A1, 1184–1411; and for osteopontin (OPN), 251–446.

The mouse set was as follows: for aggrecan, 6013–6177; for chondromodulin 1, 192–474; for Col2a1, 3713–3951; for Col9a1, 1969–2196; for Col11a2, 910–1120; for Sox5, 1775–2010; and for Sox6, 2114–2271.

Western blot analysis. Western blot analysis was performed with cell extracts from SOX-overexpressing cell lines, human MSCs, and adult human DFs. Whole cell lysates or nuclear extracts (5 μg) were separated by 5–15% sodium dodecyl sulfate–polyacrylamide gel electrophoresis and transferred to polyvinylidene difluoride filters. The filters were incubated with an anti-GFP antibody (1:200; Clontech), anti-SOX antibody mixture (1:200–1:1,000 each; Santa Cruz Biotechnology, Santa Cruz, CA, and a generous gift from Dr. Yoshihiko Yamada, National Institutes of Health, Bethesda, MD, and Dr. Tomoatsu Kimura, Toyama Medical and Pharmaceutical University, Toyama, Japan). Antigen–antibody complexes were detected with horseradish peroxidase–conjugated secondary antibodies and visualized with the use of an ECL-Plus system (Amersham, Piscataway, NJ).

Histologic analysis. Spheroids and mouse tibias were fixed overnight at 4°C in 4% paraformaldehyde/phosphate buffered saline, transferred to 70% ethyl alcohol, and stored at 4°C until they were used. Subsequently, the samples were either frozen in OCT compound and then sectioned at 10 μm or embedded in paraffin and sectioned at 5 μm. Sections were stained with Alcian blue, toluidine blue, or Safranin O to evaluate the cartilaginous matrix, and with hematoxylin and eosin to evaluate the morphology, as previously described (32). Immunohistochemistry for Col2 and LacZ was performed as previously described (32).

In vivo *SOX* gene transfer. Ten 8-week-old C57BL/6J mice were divided into 2 groups and anesthetized with an intraperitoneal injection of pentobarbiturate (5 mg/100 gm of body weight). Then, 10 μl of a suspension of adenovirus vector expressing LacZ or the SOX trio (10^8 MOI) was injected into the subcutaneous tissue in front of the anteromedial diaphysis of the tibia. The mice were killed 1 week after surgery, and the entire tibia and surrounding tissue were harvested for histologic and immunohistochemical analyses. Whole tibias were dissected and fixed for 2 hours in 4% paraformaldehyde/phosphate buffered saline, pH 7.4, and decalcified for 2 weeks

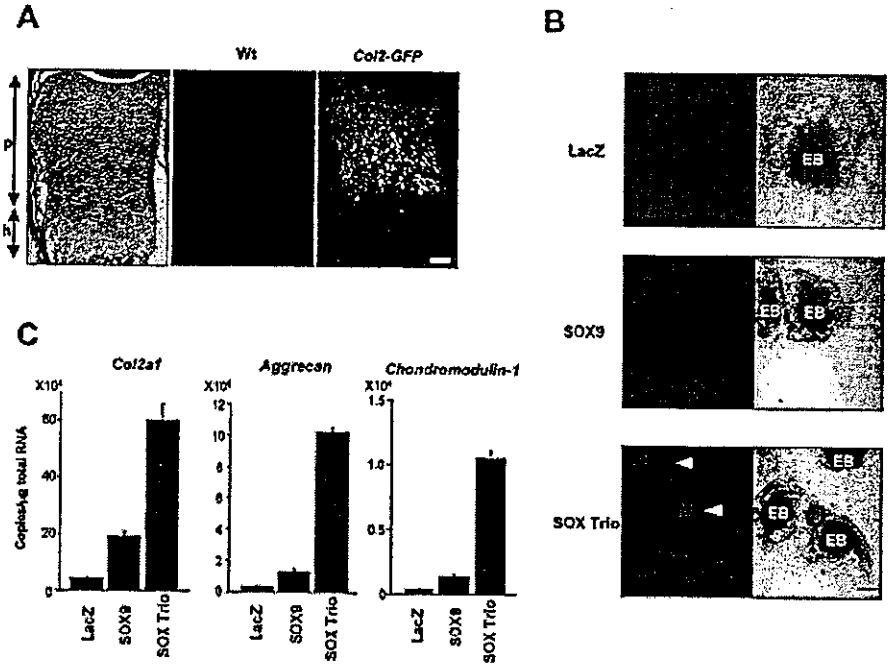

Figure 1. Induction of chondrocytic phenotypes in embryonic stem (ES) cells by the SOX trio. A, Fluorescence of growth plate chondrocytes from the *Col2-GFP*–transgenic mouse at embryonic day 18.5. The tibias from wild-type (Wt) and *Col2-GFP* neonate mice were sectioned, and the distal portions were examined by fluorescence microscopy. The morphology of the growth plate is shown at the left with hematoxylin and eosin staining. p = proliferating layer of growth plate chondrocytes; h = hypertrophic layer of growth plate chondrocytes. Bar = 100 μm. B, Fluorescence of *Col2-GFP* ES cells treated with the combination of SOX5, SOX6, and SOX9 (the SOX trio). LacZ, SOX9, or the SOX trio was adenovirally expressed in embryoid bodies (EB) of ES cells established from the *Col2-GFP*–transgenic mouse, and fluorescence was evaluated on day 3 after transduction (arrowheads). The left half of each panel shows green fluorescence protein (GFP) fluorescence; the right half shows a merging of the GFP fluorescence image and the transmitted image. Bar = 200 μm. C, Expression of the cartilage marker genes *Col2a1*, *Aggrecan*, and *Chondromodulin 1* by ES cells treated with LacZ, SOX9, or the SOX trio for 7 days. Levels of mRNA expression were analyzed by real-time polymerase chain reaction.

in 10% EDTA, pH 7.4. After processing and embedding in paraffin, 3-μm sagittal sections were cut and stained with Safranin O and fast green. Immunohistochemistry for type II collagen was performed as previously described (32).

Animal care was in accordance with the policies of the University of Tokyo School of Medicine.

GenBank sequences. Human gene sequences were obtained from GenBank (accession nos. M55172 for *AGGRECAN*, AB006000 for *CHONDROMODULIN 1*, X16468 for *COL2A1*, X54412 *COL9A1*, X60382 for *COL10A1*, NM_080679 for *COL11A2*, AJ224741 for *MATRILIN 3*, AB081589 for *SOX5*, AF309034 for *SOX6*, Z46629 for *SOX9*, NM_004348 for *RUNX2*, Z74615 for *COL1A1*, and AF052124 for *OPN*).

Mouse gene sequences were also obtained from GenBank (accession nos. L07049 for *Aggrecan*, NM_010701.1 for *Chondromodulin 1*, NM_031163 for *Col2a1*, D17511 for *Col9a1*, NM_009926 for *Col11a2*, AB006330 for *Sox5*, and U32614 for *Sox6*).

Image acquisition. An Axioskop 2 Plus (Carl Zeiss, Oberkochen, Germany) microscope was used for microscopic observation (bright and fluorescence fields at ×100, ×200, and ×400 magnifications). Photographs were taken with an AxioCam HRc (Carl Zeiss) camera, and images were acquired with AxioVision 3.0 software (Carl Zeiss).

RESULTS

Induction of cartilage marker gene expression in ES cells by the SOX trio. To screen for sufficient conditions for chondrogenesis, we needed a monitoring system that could detect chondrocyte differentiation in an easy, precise, and noninvasive manner. For this

purpose, we established transgenic mice expressing the chondrocyte-specific *Col2a1* promoter–*GFP* reporter gene and isolated totipotent, undifferentiated ES cells from them. Since GFP expression was specifically localized to the cartilage in these mice (Figure 1A), ES cells from these mice were expected to fluoresce solely upon chondrocyte differentiation. Using this system, we examined the effects of gain and loss of function of representative factors that are known to be important for chondrogenesis: SOX5, SOX6, SOX9, IGF-1, FGF-2, IHH, BMP-2, TGFβ, and Wnt proteins.

Since we intended to find factors affecting chondrocyte differentiation directly rather than indirectly, the assessment of fluorescence was done within 3 days after transduction. As a result, no single factor caused fluorescence; hence, we screened for all possible combinations of these factors. It turned out that *GFP* expression was observed only upon treatment with the combination of SOX5, SOX6, and SOX9 (the SOX trio) (Figure 1B), while there was no fluorescence upon treatment with the other combinations, including each SOX alone, within this period (results not shown).

We then examined the expression levels of the cartilage marker genes, which included the cartilaginous collagens (such as *Col2a1*, *Col9a1*, and *Col11a2*), cartilaginous proteoglycans (such as *Aggrecan*), and other cartilage-specific proteins that play key roles in maintaining cartilage structures (such as *Chondromodulin 1*) (33,34). Real-time PCR analysis confirmed that the SOX trio markedly up-regulated the levels of expression of *Col2a1*, *Aggrecan*, and *Chondromodulin 1* compared with SOX9 alone or the LacZ control (Figure 1C).

Induction of chondrocytic phenotypes in human MSCs by the SOX trio. We next examined the effect of the SOX trio on the chondrocyte differentiation of human MSCs. Expression of each SOX protein by adenoviruses was confirmed by Western blot analysis with specific antibodies (Figure 2A). To characterize human MSCs treated with SOX proteins, we evaluated the levels of expression of the cartilage marker genes by real-time PCR (Figure 2B). When cultured with serum-free DMEM in spheroids, human MSCs treated with the LacZ virus did not express detectable levels of the cartilage-specific collagen genes *COL2A1*, *COL9A1*, or *COL11A2* during 3 weeks of spheroid culture. In contrast, when the SOX trio was overexpressed, expression of these genes was detected as early as 3 days after spheroid formation. The number of copies of their mRNA continued to rise during the 3 weeks of spheroid culture. After 3 weeks of spheroid culture, the copy number of *COL2A1* mRNA from human MSCs exceeded that of *COL2A1* from the tracheal cartilage and articular cartilage.

When an individual SOX gene was transduced, expression of *COL2A1*, *COL9A1*, and *COL11A2* was not detected after 1 week of spheroid culture. After 2 weeks, only human MSCs treated with SOX9 expressed low levels of their mRNA. In contrast, *AGGRECAN* was already expressed at a moderate level even in untreated human MSCs, and its expression was substantially up-regulated by treatment with SOX9 alone or with the SOX trio after 2 weeks of spheroid culture. *CHONDROMODULIN 1* and *MATRILIN 3* were also induced by treatment with the SOX trio. The induction was first observed after 3 days of spheroid culture, and the copy number of their mRNA gradually increased up to 3 weeks.

We then performed histologic examinations of human MSCs treated with LacZ or the SOX trio and cultured in spheroids with serum-free DMEM or the chondrogenic medium containing TGFβ and BMP-2 (Figure 2C). Human MSCs treated with the SOX trio and cultured in spheroids with serum-free DMEM produced a proteoglycan-rich extracellular matrix characteristic of cartilage, which showed purple staining (metachromasia) with toluidine blue as early as 1 week after spheroid formation, whereas those treated with an individual SOX failed to show any staining at this stage. After 3 weeks, induction of proteoglycan-rich matrix by the SOX trio became more prominent. At higher magnification, cells in the spheroid were found to be completely surrounded by a proteoglycan-rich matrix, resembling the lacunar structure of cartilage (Figure 2D).

When cultured in the chondrogenic medium, accumulation of proteoglycan-rich matrix was accelerated (Figure 2C). After 1 week, the SOX trio induced abundant matrix production, whereas human MSCs treated with each SOX alone showed only weak production. After 3 weeks, although all spheroids including the LacZ control produced proteoglycan-rich matrix, human MSCs treated with the SOX trio showed the most abundant production. Staining with Alcian blue and Safranin O showed similar results (results not shown).

Production of type II collagen protein was detected by immunohistochemistry (Figure 2E). Human MSCs cultured in spheroids with the chondrogenic medium and treated with the SOX trio produced the most abundant type II collagen protein. Human MSCs cultured with serum-free DMEM and treated with the SOX trio and those cultured in the chondrogenic medium and treated with LacZ produced the second most abundant type II collagen protein. No type II collagen

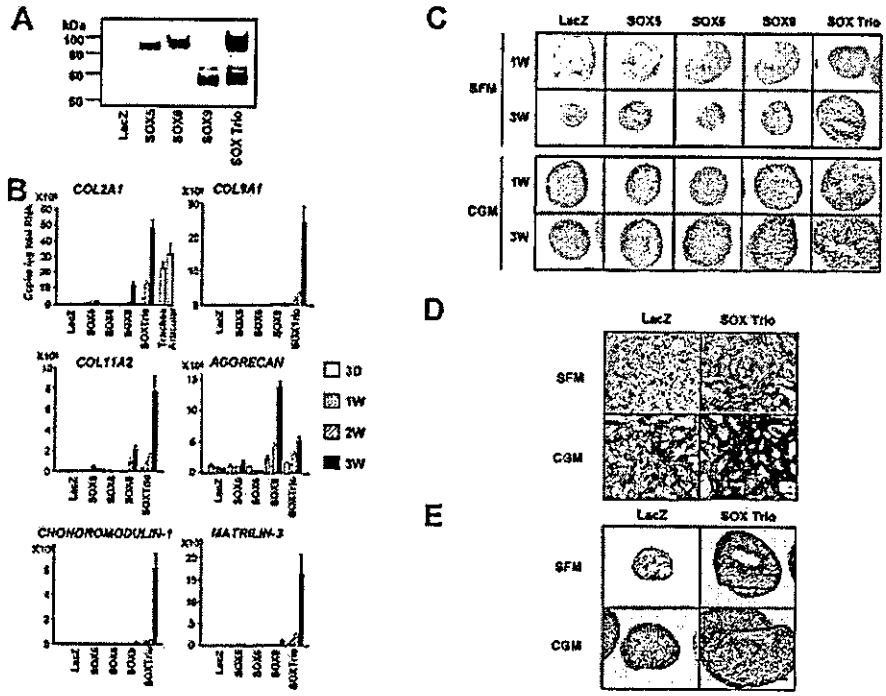

Figure 2. Induction of chondrocytic phenotypes in human mesenchymal stem cells (MSCs) by the SOX trio. A, Levels of adenovirally expressed SOX protein expression by human MSCs, as detected by Western blot analysis 5 days after transduction (expected sizes: 82 kd for SOX5, 87 kd for SOX6, and 56 kd for SOX9). B, Levels of mRNA expression of the cartilage marker genes *COL2A1*, *COL9A1*, *COL11A2*, *AGGRECAN*, *CHONDROMODULIN 1*, and *MATRILIN 3* by human MSCs. Cells were treated with LacZ, SOX5, SOX6, SOX9, or the SOX trio and cultured in spheroids with serum-free Dulbecco's modified Eagle's medium (DMEM) for 3 days, 1 week, 2 weeks, or 3 weeks, and mRNA expression was analyzed by real-time polymerase chain reaction. As positive controls, *COL2A1* mRNA levels were measured in tracheal and articular cartilage. C, Production of proteoglycan-rich matrix by human MSCs treated with LacZ, SOX5, SOX6, SOX9, or the SOX trio and cultured in spheroids with serum-free DMEM (SFM) or chondrogenic medium (CGM) for 1 week or 3 weeks. Spheroid sections were stained with toluidine blue. Proteoglycan-rich matrix stained purple (metachromasia). Bar = 100 μm. D, Higher-magnification views of proteoglycan-rich matrix produced by human MSCs treated with LacZ or the SOX trio and cultured in spheroids with SFM or CGM for 3 weeks. Spheroid sections were stained with toluidine blue. Bar = 20 μm. E, Expression of type II collagen protein by human MSCs treated with LacZ or the SOX trio and cultured in spheroids with SFM or CGM for 3 weeks. Type II collagen protein was detected by immunohistochemistry (brown staining). Bar = 100 μm.

production was observed in human MSCs cultured in spheroids with serum-free DMEM and treated with LacZ (Figure 2E). Interestingly, the presence of the chondrogenic medium did not cause an increase in mRNA levels of the cartilage marker genes (data not shown).

Induction of chondrocytic phenotypes in non-chondrogenic human immortalized cell lines by the SOX trio. So far, we had found that the SOX trio can induce chondrocytic phenotypes in totipotent ES cells and multipotent MSCs. If the SOX trio constitutes signals sufficient for the induction of chondrogenesis, it may induce chondrocytic phenotypes in cells already committed to other lineages. To test this possibility, we chose 3 human nonchondrogenic cell lines: HeLa cells derived from the cervix, HuH-7 cells derived from the liver (35), and HEK 293 cells derived from the embryonic kidney (36). Since these cell lines did not tolerate adenoviral transduction well, probably due to rapid proliferation of adenoviruses in these immortalized cells, we used plasmid transfection for gene delivery.

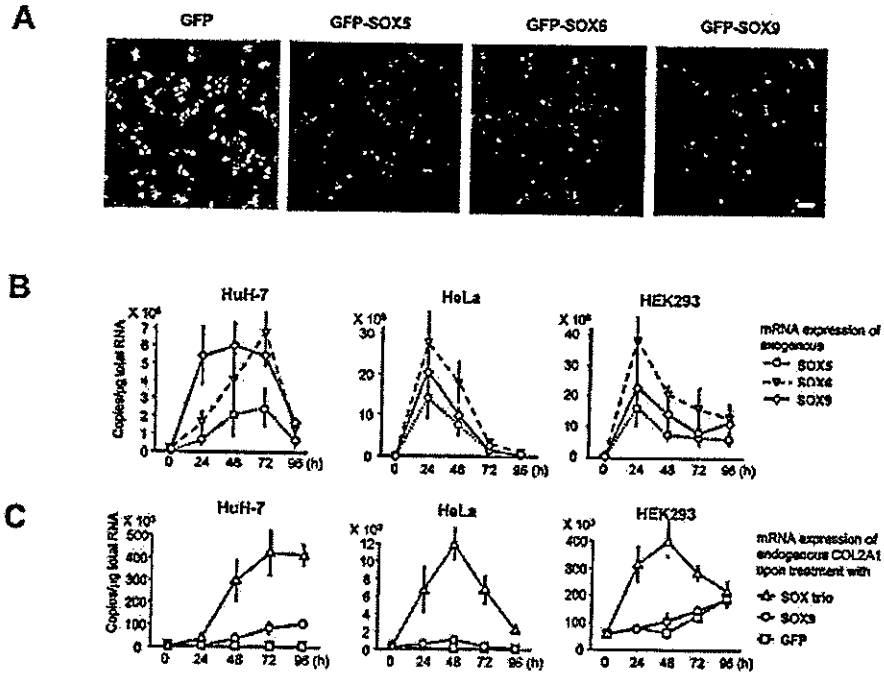

Figure 3. Induction of chondrocytic phenotypes in nonchondrogenic human cell lines by the SOX trio. A, Expression of green fluorescence protein (GFP)–tagged SOX proteins in HuH-7 cells. Each of the plasmids expressing GFP-tagged SOX genes was transiently transfected, and their expression levels and subcellular localization were detected as fluorescence using confocal fluorescence microscopy. Bar = 100 μm. B, Temporal mRNA expression profiles of exogenous SOX5, SOX6, and SOX9 in HuH-7, HEK 293, and HeLa cells transiently transfected with plasmids expressing these GFP-tagged SOX genes. Cells were cultured in monolayer with Dulbecco's modified Eagle's medium containing 10% fetal bovine serum. Levels of mRNA expression were analyzed by real-time polymerase chain reaction (PCR). C, Temporal mRNA expression profiles of endogenous *COL2A1* in HuH-7, HEK 293, and HeLa cells transfected with plasmids expressing GFP, SOX9, or the SOX trio. Levels of mRNA expression were analyzed by real-time PCR.

When each of the plasmids expressing GFP-tagged *SOX* genes was transiently transfected into these cells, each GFP-tagged SOX protein was well expressed and localized in the nuclei (Figure 3A). Real-time PCR analysis revealed that the peak expression of all SOXs was achieved at 24–72 hours after transfection (Figure 3B). The SOX trio induced *COL2A1* mRNA expression within 3 days (Figure 3C). The temporal profile of *COL2A1* up-regulation correlated well with those of the exogenous *SOX* genes. Similar results were obtained with *COL9A1* and *COL11A2* (data not shown). It is noteworthy that overexpression of SOX9 alone up-regulated *COL2A1* to some extent in HuH-7 cells expressing moderate levels of endogenous *SOX5* and *SOX6* (37), but not in HeLa cells expressing no endogenous *SOX5* or *SOX6*.

Induction of chondrocytic phenotypes in adult human DFs by the SOX trio. We further examined whether the SOX trio could induce chondrocytic phenotypes in well-differentiated primary mesenchymal cells such as adult human DFs. Since adult human DFs can be easily harvested and cultured, and grow faster than human MSCs, they could be an alternative cell source for cartilage tissue engineering. Adult human DFs treated with the SOX trio were cultured in spheroids with serum-free DMEM. The SOX trio rapidly induced *COL2A1*, *COL11A2*, *AGGRECAN*, and *MATRILIN 3* within 3 days, and their levels continued to increase for up to 3 weeks (Figure 4A). *COL9A1* and *CHONDROMODULIN 1* were induced at 7 days after spheroid formation, and their expression levels continued to rise for up to 3 weeks as well. Unlike the human MSCs, adult

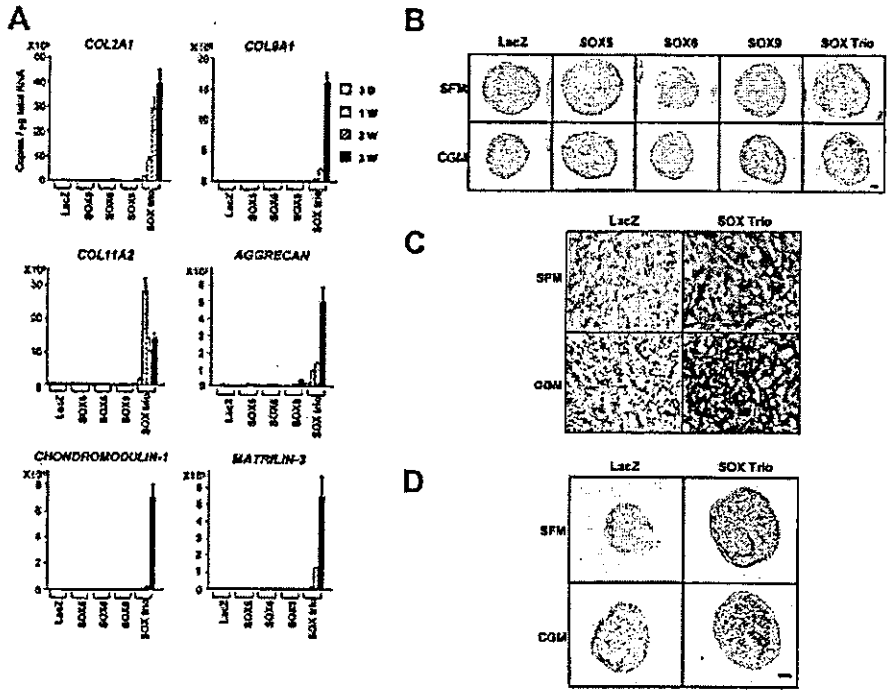

Figure 4. Induction of chondrocytic phenotypes in adult human dermal fibroblasts (DFs) by the SOX trio. **A,** Levels of mRNA expression of the cartilage marker genes *COL2A1*, *COL9A1*, *COL11A2*, *AGGRECAN*, *CHONDROMODULIN 1*, and *MATRILIN 3* by adult human DFs. Cells were treated with LacZ, SOX5, SOX6, SOX9, or the SOX trio and cultured in spheroids with serum-free Dulbecco's modified Eagle's medium (DMEM) for 3 days, 1 week, 2 weeks, or 3 weeks, and mRNA expression was analyzed by real-time polymerase chain reaction. **B,** Production of proteoglycan-rich matrix by adult human DFs treated with LacZ, SOX5, SOX6, SOX9, or the SOX trio and cultured in spheroids with serum-free DMEM (SFM) or chondrogenic medium (CGM) for 3 weeks. Proteoglycan-rich matrix stained purple (metachromasia) with toluidine blue. **C,** Higher-magnification views of proteoglycan-rich matrix produced by adult human DFs treated with LacZ or the SOX trio and cultured in spheroids with serum-free DMEM or chondrogenic medium for 3 weeks. Spheroid sections were stained with toluidine blue. Bar = 20 μm. **D,** Expression of type II collagen protein by adult human DFs treated with LacZ or the SOX trio and cultured in spheroids with serum-free DMEM or chondrogenic medium for 3 weeks. Type II collagen protein was detected with immunohistochemistry (brown staining). Bar = 100 μm.

human DFs showed low basal expression of the cartilage marker genes, and treatment with SOX9 alone resulted in very weak or no induction. We compared mRNA expression levels of the cartilage marker genes by adult human DFs and human MSCs that were treated with the SOX trio and cultured in spheroids with serum-free DMEM up to 3 weeks, and found them to be comparable (data not shown).

When cultured in spheroids with serum-free DMEM for 3 weeks, adult human DFs treated with the SOX trio exhibited an accumulation of proteoglycan-rich matrix, whereas those treated with LacZ or with each SOX alone did not (Figure 4B). When cultured with the chondrogenic medium for 3 weeks, adult human DFs treated with the SOX trio further increased the production of proteoglycan-rich matrix. At higher magnification, cells in the spheroid were found to be surrounded by proteoglycan-rich matrix, resembling the lacunar structure of cartilage (Figure 4C). Adult human DFs treated with SOX9 alone showed weak, focal production of proteoglycan-rich matrix in the presence of the chondrogenic medium, whereas those treated with LacZ, SOX5, or SOX6 did not (Figure 4B). Production of type II collagen protein by adult human DFs treated with the SOX trio and cultured with serum-free DMEM or the chondrogenic medium was confirmed by immunohistochemistry, whereas those treated with LacZ and cultured with serum-free DMEM or the chondrogenic

medium did not exhibit any immunoreactivity (Figure 4D). As with the human MSCs, the presence of the chondrogenic medium did not cause an increase in mRNA levels of the cartilage marker genes (data not shown).

Influence of different culture systems on the induction of chondrocytic phenotypes by the SOX trio. We next examined the effect of different culture systems on chondrocyte differentiation induced by the SOX trio. Three-dimensional cell–cell interactions and the extracellular matrix are known to influence the differentiation potentials of many cell types. Monolayer culture has been reported to be disadvantageous to chondrocyte differentiation, and therefore, spheroid culture and 3-D culture are preferable (38). If the SOX trio provides signals sufficient for chondrogenesis, it may obviate the need for these specific culture formats. To test this possibility, we compared the expression levels of the cartilage marker genes *COL2A1*, *AGGRECAN*, and *CHONDROMODULIN 1* by human MSCs cultured with serum-free DMEM in monolayer, in spheroids, and in 3-D collagen. Even in monolayer culture, treatment with the SOX trio induced high levels of the cartilage marker genes within 1–2 weeks, and their expression levels increased for up to 3 weeks (data not shown). Peak expression levels of the cartilage marker genes in monolayer culture were comparable to those in spheroid culture. Similar results were obtained with adult human DFs (data not shown).

Levels of expression of the cartilage marker genes by human MSCs and adult human DFs treated with the SOX trio and cultured with serum-free DMEM in 3-D collagen cultures were much higher than those cultured in spheroid or monolayer cultures (data not shown), and there was substantial accumulation of proteoglycan-rich matrix secreted into the collagen gel (data not shown).

Induction of the expression of *SOX5* and *SOX6* in vitro by SOX9. Conditional ablation of *Sox9* was shown to cause a marked down-regulation of *Sox5* and *Sox6* mRNA expression (19), strongly suggesting that *Sox9* is necessary for the expression of *Sox5* and *Sox6*. In our experiments, ES cells, human MSCs, and adult human DFs treated with SOX9 alone started to express low levels of some cartilage marker genes after 2 weeks of culture, suggesting the formation of the SOX trio at a later period (Figures 2 and 4). Taken together, it is likely that SOX9 may induce the expression of *SOX5* and *SOX6*, but the hypothesis has never been directly proven. In our experiment, human MSCs treated with SOX9 alone and cultured with serum-free DMEM in 3-D collagen for 1 week began to express *SOX5* and *SOX6* mRNA, whereas those treated with LacZ and cultured with serum-free DMEM in 3-D collagen did not (Figure 5A). This is the first direct proof that SOX9 induces *SOX5* and *SOX6*. We also demonstrated that *SOX5* and *SOX6* did not induce each other. Similar results were obtained with ES cells and adult human DFs (data not shown). This induction was also seen in monolayer or spheroid culture, but the degree of up-regulation was smaller and took 2–3 weeks (data not shown).

Suppression of hypertrophic and osteogenic markers by the SOX trio. In human MSCs, mRNA for the gene encoding the type X collagen α1 chain (*COL10A1*), a marker for hypertrophic chondrocytes, was up-regulated when it were cultured in the chondrogenic medium in spheroids (39). Levels of mRNA expression of hypertrophic and osteogenic marker genes, such as *COL10A1*, *RUNX2*, *OPN*, and *COL1A1*, were markedly increased in 3-D collagen culture with serum-free DMEM (Figure 5B). Treatment with SOX9 alone failed to suppress these genes except for *COL1A1*, whereas treatment with the SOX trio suppressed all of these genes (Figure 5B). In adult human DFs cultured in 3-D collagen with serum-free DMEM, there was no induction of hypertrophic or osteogenic marker genes, regardless of treatment with the SOX trio (data not shown).

In vivo induction of cartilage-like tissue by the SOX trio. To test whether the SOX trio could influence cartilage formation in vivo, we directly introduced the SOX trio genes in the subcutaneous tissue. Adenoviruses expressing the SOX trio were injected into the subcutaneous tissue lying above the tibia, and 1 week after treatment, the mice were killed, and the tissues were harvested and analyzed histologically and immunohistochemically. The viruses transduced subcutaneous cells efficiently, as shown by the positive staining for LacZ immunoreactivity (Figure 5C). In all 5 mice treated with the SOX trio, chondrocyte-like cells appeared in the area adjacent to the bone. These cells stained positive for Safranin O and type II collagen immunoreactivity (Figure 5D). In contrast, no such cells were seen in the 5 mice that were treated with LacZ.

DISCUSSION

In our screening combinations of factors that are known to be necessary for chondrogenesis, we found that the SOX trio induced chondrocytic phenotypes in totipotent ES cells within 3 days. Previous studies of

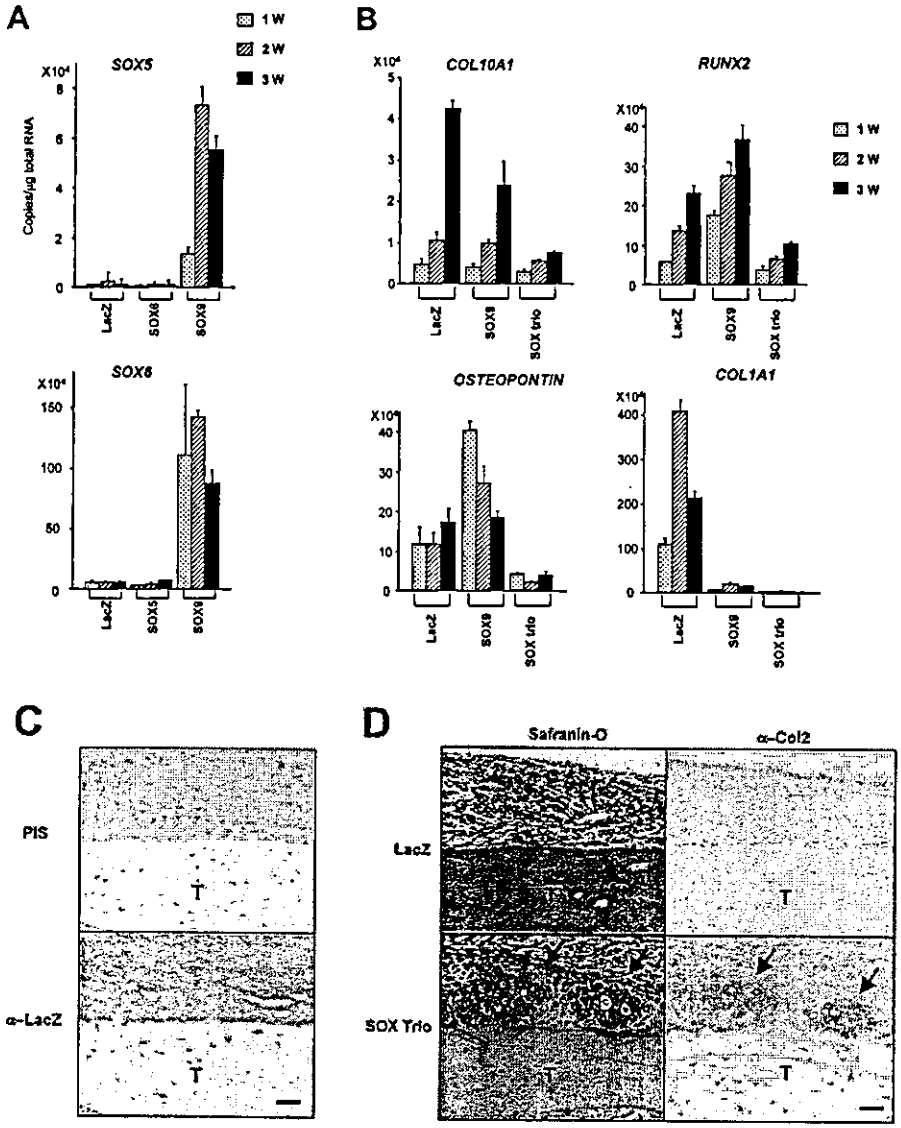

Figure 5. Induction of *Sox5* and *Sox6* expression by SOX9, suppression of hypertrophic and osteogenic differentiation by the SOX trio, and in vivo induction of cartilaginous tissue by the SOX trio. **A**, Levels of mRNA expression of *SOX5* and *SOX6* in human MSCs treated with LacZ, SOX5, SOX6, or SOX9 and cultured in 3-dimensional (3-D) collagen with serum-free Dulbecco's modified Eagle's medium (DMEM) for 1, 2, or 3 weeks, and mRNA expression levels were analyzed by real-time polymerase chain reaction (PCR). **B**, Levels of mRNA expression of the hypertrophic and osteogenic markers *COL10A1*, *RUNX2*, *OSTEOPONTIN*, and *COL1A1* by human MSCs treated with LacZ, SOX9, or the SOX trio and cultured in 3-D collagen with serum-free DMEM for 1, 2, or 3 weeks. Levels of mRNA expression were analyzed by real-time PCR. **C**, Adenoviruses expressing LacZ or the SOX trio were directly injected into the subcutaneous tissue lying above the anteromedial diaphysis of the tibia (T) and the transduction efficiency of adenoviruses was detected by immunohistochemistry for LacZ. Sections were treated with preimmune serum (PIS) or anti-LacZ antibody (α-LacZ). LacZ protein stained brown. Bar = 100 μm. **D**, Production of proteoglycan-rich matrix and induction of type II collagen protein by the SOX trio. Sections were stained with Safranin O and fast green; cartilage (arrows) stained orange. Type II collagen protein (arrows) was detected by immunohistochemistry (brown staining) with anti-type II collagen antibody (α-Col2). Bar = 100 μm.

human MSCs showed that treatment with the chondrogenic supplements TGFβ, BMP-2, or both for 2–3 weeks could induce chondrocytic phenotypes (39,40). In the present study, the SOX trio successfully induced chondrocytic phenotypes in human MSCs cultured in serum-free DMEM containing no supplements. Moreover, human MSCs treated with the SOX trio expressed the cartilage marker genes more rapidly and more potently than did those treated with the conventional chondrogenic method, and their levels of mRNA expression induced by the SOX trio were independent of the presence of TGFβ and BMP-2. These findings raised the possibility that the SOX trio may provide signals sufficient for the induction of chondrogenesis.

We found that the SOX trio induced cartilage-specific genes that did not belong to collagens or proteoglycans: *MATRILIN 3* and *CHONDROMODULIN 1*. Expression of *MATRILIN 3* is highly specific for cartilage (33). Mutations in *MATRILIN 3* cause a type of human chondrodysplasia known as multiple epiphyseal dysplasia, which is characterized by early-onset heritable osteoarthritis (33). Expression of *CHONDROMODULIN 1* is also specific for cartilage. *CHONDROMODULIN 1* stimulates chondrocyte proteoglycan synthesis and inhibits capillary network formation (34,41). The induction of these genes as well as cartilaginous collagens and proteoglycans by the SOX trio further supports the notion that the SOX trio may provide sufficient signals for the induction of chondrogenesis.

A recent study revealed that in vitro chondrogenesis of murine bone marrow–derived MSCs was enhanced by the overexpression of SOX9 (42). Our data with human MSCs partially support this, in that the cartilage marker genes (*COL2A1*, *COL11A2*, and *AGGRECAN*) were induced in human MSCs treated with SOX9 alone. However, the levels of *COL2A1* and *COL11A2* expression were much lower than those induced in human MSCs treated with the SOX trio. In addition, *COL9A1*, *MATRILIN 3*, and *CHONDROMODULIN 1* were only slightly induced by treatment with SOX9 alone. These findings suggest that SOX9 alone is not sufficient for the induction of chondrogenesis and further emphasizes the importance of the SOX trio.

Although treatment with the SOX trio successfully induced mRNA expression of the cartilage marker genes to a level comparable to that in normal cartilage and induced the production of proteoglycan-rich matrix, the addition of the chondrogenic medium containing TGFβ and BMP-2 further increased the accumulation of proteoglycan-rich matrix without increasing the mRNA expression of the cartilage marker genes in both human MSCs and adult human DFs. Thus, TGFβ and BMP-2 may induce other genes that are important for matrix accumulation, or they may be working at the posttranscriptional level. It is noteworthy that in adult human DFs, the chondrogenic medium had no effect on the production of proteoglycan-rich matrix in the absence of treatment with the SOX trio, whereas in human MSCs, the chondrogenic medium had some positive effect in the absence of treatment with the SOX trio. This difference seems to be due to some basal expression of the SOX genes in human MSCs and underscores the important role of the SOX trio in chondrogenesis. The exact mechanism(s) by which TGFβ and BMP-2 increase the accumulation of proteoglycan-rich matrix needs to be further investigated and a gene array analysis performed.

Since human MSCs consist of early mesenchymal progenitors that are already committed to some extent, there is a possibility that the SOX trio may merely be expanding the existing chondroprogenitors by increasing their proliferation or suppressing their cell death, rather than directly inducing chondrocytic phenotypes of non-committed cells. To rule out this possibility, the SOX trio was introduced into cell types other than human MSCs. The SOX trio was able to induce chondrocytic phenotypes in ES cells, which are uncommitted and undifferentiated, as well as in cells belonging to other lineages, such as immortalized cell lines derived from the kidney, liver, and cervix. The SOX trio also successfully induced chondrocytic phenotypes in adult human DFs cultured with serum-free DMEM. Expression levels of the cartilage marker genes induced by the SOX trio in adult human DFs were comparable to those in human MSCs induced by the SOX trio and were also independent of treatment with the chondrogenic medium. These findings strongly suggest that expression of the SOX trio is indeed sufficient for the induction of chondrogenesis.

The SOX trio induced chondrocytic phenotypes in cells cultured in monolayer as effectively as in cells in spheroid culture. Since the monolayer culture is usually disadvantageous for in vitro chondrogenesis and since primary chondrocytes cultured in monolayer quickly lose chondrocytic phenotypes through a process known as dedifferentiation, the conventional in vitro chondrogenic methods invariably use spheroid culture or 3-D culture. It is likely that spheroid culture and 3-D culture may provide some unknown signals that are necessary for chondrogenesis but are not present in monolayer culture. The fact that the SOX trio obviated the use of

spheroid culture further supports the importance of the SOX trio in chondrogenesis. At the same time, it shows the limitation of the SOX trio, since the results did not fully match those obtained with the 3-D culture.

We found that the SOX trio helped to maintain the phenotype of permanent cartilage by suppressing the expression of the marker genes for hypertrophic and osteogenic differentiation, which were induced with the conventional chondrogenic method. This finding may reflect in vivo reciprocal expression patterns of the SOX trio and hypertrophic/osteogenic marker genes (21) and enlargement of the hypertrophic zone in the epiphyseal growth plate of $Sox9^{+/-}$ mice (43). Although the mechanism of the down-regulation is not yet clear, the SOX trio may directly inhibit hypertrophic and osteogenic markers. Alternatively, proteins such as chondromodulin 1 induced by the SOX trio may down-regulate these markers. In either case, inhibition of hypertrophic and osteogenic markers by the SOX trio is compatible with the notion that the SOX trio directly induces chondrocyte differentiation, and this finding is advantageous for tissue engineering of articular, facial, and tracheal cartilage, which needs to remain nonhypertrophic and nonosteogenic.

This is the first study to show that SOX9 induces *SOX5* and *SOX6*. When treated with SOX9, both human MSCs and adult human DFs began to express *SOX5* and *SOX6* at 1 week after transduction. This finding fits the in vivo sequential expression patterns of *SOX5*, *SOX6*, and *SOX9* and is compatible with the previously reported data (19) that $Sox9^{flox/flox}$, *Prx1-Cre*, and *Col2a1-Cre* mice lost the expression of *Sox5* and *Sox6* in cells that lacked SOX9. This finding is also compatible with our observation that overexpression of SOX9 alone up-regulated cartilage marker genes to some extent in HuH-7 cells expressing moderate levels of endogenous *SOX5* and *SOX6*, but not in HeLa cells expressing no endogenous *SOX5* or *SOX6*. These observations further stress the importance of the SOX trio over individual SOXs in the induction of chondrocytic phenotypes. The mechanism of *SOX5* and *SOX6* induction by SOX9 should be further investigated by analyzing human MSCs and adult human DFs treated with SOX9 alone.

When the SOX trio was adenovirally expressed in the subcutaneous tissue, new cartilage formation was induced. Although the adenoviruses infected most of the cells in the injected area, the strongest induction was observed in the area adjacent to the bone, including the periosteum. This finding suggests that despite the strong chondrogenic actions of the SOX trio, there are cells in the periosteal region that are more susceptible to the signal. These cells may represent an enrichment of MSCs in the perichondrium.

In conclusion, the findings of the current study strongly suggest that the SOX trio provides signals that are sufficient for the induction of permanent cartilage in vitro. The potent in vitro chondrogenic system of the SOX trio provides a new in vitro model of chondrogenesis, which may help us to better understand the mechanism of chondrogenesis and to advance cartilage regenerative medicine.

ACKNOWLEDGMENTS

We thank Drs. Yoshihiko Yamada and Tomoatsu Kimura for the generous gift of SOX9 antibodies, and Ms Aya Narita, Tomoko Kusadokoro, and Mizue Ikeuchi for technical assistance.

REFERENCES

1. De Crombrugghe B, Lefebvre V, Nakashima K. Regulatory mechanisms in the pathways of cartilage and bone formation. Curr Opin Cell Biol 2001;13:721–7.
2. Kolettas E, Muir HI, Barrett JC, Hardingham TE. Chondrocyte phenotype and cell survival are regulated by culture conditions and by specific cytokines through the expression of Sox-9 transcription factor. Rheumatology (Oxford) 2001;40:1146–56.
3. Stheneur C, Dumontier MF, Guedes C, Fulchignoni-Lataud MD, Tahiri K, Karensty G, et al. Basic fibroblast growth factor as a selective inducer of matrix Gla protein gene expression in proliferative chondrocytes. Biochem J 2003;369:63–70.
4. Church VL, Francis-West P. Wnt signalling during limb development. Int J Dev Biol 2002;46:927–36.
5. Zehentner BK, Dony C, Burtscher H. The transcription factor Sox9 is involved in BMP-2 signaling. J Bone Miner Res 1999;14:1734–41.
6. Tuli R, Tuli S, Nandi S, Wang ML, Alexander PG, Haleem-Smith H, et al. Transforming growth factor-β-mediated chondrogenesis of human mesenchymal progenitor cells involves N-cadherin and mitogen-activated protein kinase and Wnt signaling cross-talk. J Biol Chem 2003;278:41227–36.
7. Ng LJ, Wheatley S, Muscat GE, Conway-Campbell J, Bowles J, Wright E, et al. SOX9 binds DNA, activates transcription, and coexpresses with type II collagen during chondrogenesis in the mouse. Dev Biol 1997;183:108–21.
8. Zhao Q, Eberspaecher H, Lefebvre V, de Crombrugghe B. Parallel expression of Sox9 and Col2a1 in cells undergoing chondrogenesis. Dev Dyn 1997;209:377–86.
9. Foster JW, Dominguez-Steglich MA, Guioli S, Kowk G, Weller PA, Stevanovic M, et al. Campomelic dysplasia and autosomal sex reversal caused by mutations in an SRY-related gene. Nature 1994;372:525–30.
10. Wagner T, Wirth J, Meyer J, Zabel B, Held M, Zimmer J, et al. Autosomal sex reversal and campomelic dysplasia are caused by mutations in and around the SRY-related gene SOX9. Cell 1994;79:1111–20.
11. Bi W, Deng JM, Zhang Z, Behringer RR, de Crombrugghe B. Sox9 is required for cartilage formation. Nat Genet 1999;22:85–9.
12. Bell DM, Leung KK, Wheatley SC, Ng LJ, Zhou S, Ling KW, et al. SOX9 directly regulates the type-II collagen gene. Nat Genet 1997;16:174–8.
13. Bridgewater LC, Lefebvre V, de Crombrugghe B. Chondrocyte-

specific enhancer elements in the Col11a2 gene resemble the Col2a1 tissue-specific enhancer. J Biol Chem 1998;273: 14998–5006.
14. Lefebvre V, Huang W, Harley VR, Goodfellow PN, de Crombrugghe B. SOX9 is a potent activator of the chondrocyte-specific enhancer of the proα(II) collagen gene. Mol Cell Biol 1997;17: 2336–46.
15. Liu Y, Li H, Tanaka K, Tsumaki N, Yamada Y. Identification of an enhancer sequence within the first intron required for cartilage-specific transcription of the α2(XI) collagen gene. J Biol Chem 2000;275:12712–8.
16. Sekiya I, Tsuji K, Koopman P, Watanabe H, Yamada Y, Shinomiya K, et al. SOX9 enhances aggrecan gene promoter/enhancer activity and is up-regulated by retinoic acid in a cartilage-derived cell line, TC6. J Biol Chem 2000;275:10738–44.
17. Xie WF, Zhang X, Sakano S, Lefebvre V, Sandell LJ. Transactivation of the mouse cartilage-derived retinoic acid-sensitive protein gene by Sox9. J Bone Miner Res 1999;14:757–63.
18. Zhang P, Jimenez SA, Stokes DG. Regulation of human COL9A1 gene expression. Activation of the proximal promoter region by SOX9. J Biol Chem 2003;278:117–23.
19. Akiyama H, Chaboissier MC, Martin JF, Schedl A, de Crombrugghe B. The transcription factor Sox9 has essential roles in successive steps of the chondrocyte differentiation pathway and is required for expression of Sox5 and Sox6. Genes Dev 2002;16: 2813–28.
20. Smits P, Li P, Mandel J, Deng JM, Behringer RR, de Crombrugghe B, et al. The transcription factors L-Sox5 and Sox6 are essential for cartilage formation. Dev Cell 2001;1:277–90.
21. Lefebvre V, Li P, de Crombrugghe B. A new long form of Sox5 (L-Sox5), Sox6 and Sox9 are coexpressed in chondrogenesis and cooperatively activate the type II collagen gene. EMBO J 1998; 17:5718–33.
22. Miyagishi M, Taira K. RNAi expression vectors in mammalian cells. Methods Mol Biol 2004;252:483–91.
23. Matsumoto M, Ogawa W, Teshigawara K, Inoue H, Miyake K, Sakaue H, et al. Role of the insulin receptor substrate 1 and phosphatidylinositol 3-kinase signaling pathway in insulin-induced expression of sterol regulatory element binding protein 1c and glucokinase genes in rat hepatocytes. Diabetes 2002;51:1672–80.
24. Yamanaka Y, Tanaka H, Koike M, Nishimura R, Seino Y. PTHrP rescues ATDC5 cells from apoptosis induced by FGF receptor 3 mutation. J Bone Miner Res 2003;18:1395–403.
25. Long F, Zhang XM, Karp S, Yang Y, McMahon AP. Genetic manipulation of hedgehog signaling in the endochondral skeleton reveals a direct role in the regulation of chondrocyte proliferation. Development 2001;128:5099–108.
26. Ruiz i Altaba A. Gli proteins encode context-dependent positive and negative functions: implications for development and disease. Development 1999;126:3205–16.
27. Fujii M, Takeda K, Imamura T, Aoki H, Sampath TK, Enomoto S, et al. Roles of bone morphogenetic protein type I receptors and Smad proteins in osteoblast and chondroblast differentiation. Mol Biol Cell 1999;10:3801–13.
28. Vleminckx K, Kemler R, Hecht A. The C-terminal transactivation domain of β-catenin is necessary and sufficient for signaling by the LEF-1/β-catenin complex in Xenopus laevis. Mech Dev 1999;81: 65–74.
29. Chung UI, Lanske B, Lee K, Li E, Kronenberg H. The parathyroid hormone/parathyroid hormone-related peptide receptor coordinates endochondral bone development by directly controlling chondrocyte differentiation. Proc Natl Acad Sci U S A 1998;95: 13030–5.
30. Robertson EJ. Embryoid-derived stem cell lines. In: Robertson EJ, editor. Teratocarcinomas and embryonic stem cells. 1st ed. Oxford: IRL Press; 1987. p. 71–112.
31. Rossert J, Eberspaecher H, de Crombrugghe B. Separate cis-acting DNA elements of the mouse pro-α1(I) collagen promoter direct expression of reporter genes to different type I collagen-producing cells in transgenic mice. J Cell Biol 1995;129:1421–32.
32. Hoshi K, Komori T, Ozawa H. Morphological characterization of skeletal cells in Cbfa1-deficient mice. Bone 1999;25:639–51.
33. Chapman KL, Mortier GR, Chapman K, Loughlin J, Grant ME, Briggs MD. Mutations in the region encoding the von Willebrand factor A domain of matrilin-3 are associated with multiple epiphyseal dysplasia. Nat Genet 2001;28:393–6.
34. Shukunami C, Hiraki Y. Expression of cartilage-specific functional matrix chondromodulin-I mRNA in rabbit growth plate chondrocytes and its responsiveness to growth stimuli in vitro. Biochem Biophys Res Commun 1998;249:885–90.
35. Nakabayashi H, Taketa K, Miyano K, Yamane T, Sato J. Growth of human hepatoma cells lines with differentiated functions in chemically defined medium. Cancer Res 1982;42:3858–63.
36. Graham FL, Smiley J, Russell WC, Nairn R. Characteristics of a human cell line transformed by DNA from human adenovirus type 5. J Gen Virol 1977;36:59–74.
37. Ikeda T, Zhang J, Chano T, Mabuchi A, Fukuda A, Kawaguchi H, et al. Identification and characterization of the human long form of Sox5 (L-SOX5) gene. Gene 2002;298:59–68.
38. Benya PD, Shaffer JD. Dedifferentiated chondrocytes reexpress the differentiated collagen phenotype when cultured in agarose gels. Cell 1982;30:215–24.
39. Sekiya I, Vuoristo JT, Larson BL, Prockop DJ. In vitro cartilage formation by adult human stem cells from bone marrow stroma defines the sequence of cellular and molecular events during chondrogenesis. Proc Natl Acad Sci U S A 2002;99:4397–402.
40. Pittenger MF, Mackay AM, Beck SC, Jaiswal RK, Douglas R, Mosca JD, et al. Multilineage potential of adult human mesenchymal stem cells. Science 1999;284:143–7.
41. Hiraki Y, Mitsui K, Endo N, Takahashi K, Hayami T, Inoue H, et al. Molecular cloning of human chondromodulin-I, a cartilage-derived growth modulating factor, and its expression in Chinese hamster ovary cells. Eur J Biochem 1999;260:869–78.
42. Tsuchiya H, Kitoh H, Sugiura F, Ishiguro N. Chondrogenesis enhanced by overexpression of sox9 gene in mouse bone marrow-derived mesenchymal stem cells. Biochem Biophys Res Commun 2003;301:338–43.
43. Bi W, Huang W, Whitworth DJ, Deng JM, Zhang Z, Behringer RR, et al. Haploinsufficiency of Sox9 results in defective cartilage primordia and premature skeletal mineralization. Proc Natl Acad Sci U S A 2001;98:6698–703.

特集II　Osteoimmunologyに関する最近の進歩と治療への応用

軟骨細胞保護におけるIL-4の役割*

西田圭一郎**
依光正則**
土井英之**
井上　一***
清水　晃****

Key Words：chondrocyte, mechanical stress, interleukin-4, osteoarthritis

はじめに

関節軟骨は唯一の基質産生細胞である軟骨細胞によって維持される結合組織であり，神経，血管，リンパ管を欠くため，軟骨細胞は関節液によって栄養を受ける．軟骨細胞が正常な代謝を営むためには，関節運動による適度な力学的負荷がかかることが必須であり，これには軟骨下の骨構造の適合性，関節液を介した関節潤滑はもちろん，筋腱あるいは靱帯のバランスによって関節が安定している必要がある．これらの条件の質的・構造的破綻は，軟骨細胞の代謝異常を招来し，変形性関節症(OA)に代表される関節炎症，軟骨破壊へと進展していく．

一方，IL-4はB細胞，T細胞，肥満細胞，マクロファージといった主に免疫，アレルギーに関与する細胞に働く多面性をもったサイトカインである．近年，軟骨細胞は正常状態でIL-4を発現，産生しており[1]，膜表面のインテグリンを介したメカニカルストレスに対する反応に関与することがわかってきた．本稿では，軟骨細胞におけるメカニカルストレス，炎症性サイトカインに対するIL-4の効果について概説する．

メカニカルストレスに対する細胞の応答とIL-4の役割

われわれはエジンバラ大学との共同研究で，Dish上で単層培養したヒト軟骨細胞に，0.33Hz，16kPaの伸張負荷をかけると約20分間で細胞膜の過分極が生じること，これが細胞膜上の$\alpha_5\beta_1$インテグリンを介したものであることを報告した[2]．さらにこの膜電位の変化はneomycin, flunarizine, N-6(aminohexyl)-5-chloro-1-naphthalene sulphonamide, genistein, staurosporine, cytochalasin Dによって阻害されることから，それぞれphospholipase C，イノシトール3リン酸を介するCa^{2+}遊離，カルモデュリン，チロシンキナーゼ，protein kinase C，細胞骨格が関与する反応であることがわかった．さらに刺激後1分でpaxillin, β-cathenin, pp125FAKなどがチロシンリン酸化を受けること，このチロシンリン酸化はRGD配列を含むオリゴ蛋白で阻害されることから，$\alpha_5\beta_1$インテグリンを介した機械的刺激に細胞骨格関連蛋白を介するシグナル伝達が必須であることも判明した．興味深いことに，刺激後の培養液を無刺激の細胞に添加することで，やはり細胞膜の過分極が誘導されることから，なん

* The role of IL-4 in regulation of chondrocyte metabolism.
** Keiichiro NISHIDA, M.D., Masanori YORIMITSU, M.D. & Hideyuki DOI, M.D.: 岡山大学大学院医歯学総合研究科機能再生・再建科学〔〒700-8558 岡山市鹿田町2-5-1〕; Department of Orthopaedic Surgery, Okayama University Graduate School of Medicine and Dentistry, Okayama 700-8558, JAPAN
*** Hajime INOUE, M.D.: 国立大学法人岡山大学
**** Akira SHIMIZU, M.D.: 愛媛大学医学部整形外科